

Meereswissenschaftliche Berichte

Marine Science Reports



No 116 2021

Megacity's fingerprint in Chinese marginal seas.

Joanna J. Waniek, Detlef E. Schulz-Bull, Birgit Gaye, Ralf Ebinghaus,
Friederike Kunz, Thomas Pohlmann, Kay-Christian Emeis (eds.)

"Meereswissenschaftliche Berichte" veröffentlichen Monographien und Ergebnisberichte von Mitarbeitern des Leibniz-Instituts für Ostseeforschung Warnemünde und ihren Kooperationspartnern. Die Hefte erscheinen in unregelmäßiger Folge und in fortlaufender Nummerierung. Für den Inhalt sind allein die Autoren verantwortlich.

"Marine Science Reports" publishes monographs and data reports written by scientists of the Leibniz-Institute for Baltic Sea Research Warnemünde and their co-workers. Volumes are published at irregular intervals and numbered consecutively. The content is entirely in the responsibility of the authors.

Schriftleitung / Editorship: Dr. Sandra Kube
(sandra.kube@io-warnemuende.de)

Die elektronische Version ist verfügbar unter / The electronic version is available on:
<http://www.io-warnemuende.de/meereswissenschaftliche-berichte.html>



© Dieses Werk ist lizenziert unter einer Creative Commons Lizenz CC BY-NC-ND 4.0 International. Mit dieser Lizenz sind die Verbreitung und das Teilen erlaubt unter den Bedingungen: Namensnennung - Nichtkommerziell - Keine Bearbeitung.

© This work is distributed under the Creative Commons License which permits to copy and redistribute the material in any medium or format, requiring attribution to the original author, but no derivatives and no commercial use is allowed, see:
<http://creativecommons.org/licenses/by-nc-nd/4.0/>

ISSN 2195-657X

Joanna J. Waniek¹, Detlef E. Schulz-Bull¹, Birgit Gaye², Ralf Ebinghaus³, Friederike Kunz¹, Thomas Pohlmann⁴, Kay-Christian Emeis^{2,3} (eds): Megacity's fingerprint in Chinese marginal seas. Meereswiss. Ber., Warnemünde, 116 (2021), doi:10.12754/msr-2021-0116

¹Leibniz Institute for Baltic Sea Research, Seestraße 15, D-18119 Rostock-Warnemünde, Germany; ²Institute of Geology, University of Hamburg, Bundesstraße 55, 20146 Hamburg, Germany; ³Institute of Coastal Research, Helmholtz-Zentrum Geesthacht Centre for Materials and Coastal Research, Max-Planck-Straße 1, 21502 Geesthacht, Germany; ⁴Institute of Oceanography, University of Hamburg, Bundesstr. 53, 20146 Hamburg, Germany

Corresponding author: joanna.waniek@io-warnemuende.de

Meereswissenschaftliche Berichte

Marine Science Reports

No. 116

Megacity's fingerprint in Chinese marginal seas

Joanna J. Waniek¹, Detlef E. Schulz-Bull¹, Birgit Gaye², Ralf Ebinghaus³, Friederike Kunz¹, Thomas Pohlmann⁴, Kay-Christian Emeis^{2,3}, Lutz Ahrens⁵, Christina Apel^{3,6}, Jana-Sophie Appelt¹, Helge W. Arz¹, Célia P. M. Bento³, Kaixuan Chen⁷, Yunru Chen⁸, Zi Cheng⁷, Kirstin Dähnke³, Carina Deich¹, Olaf Dellwig¹, Kathrin Fisch¹, Helena C. Frazão¹, Chuancheng Fu^{9,10}, Huayang Gan¹², Yonghui Gao⁷, Patrick Grunert¹¹, Chao Guo⁹, Ines Hand¹, Gaowen He^{12,13}, Tamara Hechemer¹¹, Mengxi Hu¹², Hanna Joerss³, Jérôme Kaiser¹, Marion Kanwischer¹, Niko Lahajnar², Ji Li⁷, Lianzhen Li⁹, Pingyuan Li¹², Wenguo Li⁴, Yanan Li^{9,14}, Yanfang Li^{9,15}, Yuan Li⁹, Lin Liu^{9,14,16}, Ying Liu⁹, Jianfei Lu¹², Yongming Luo^{9,10}, Jan Maier², Bernhard Mayer⁴, Frank Menger⁵, Tanja Naumann³, Yugen Ni^{12,13}, Carolin Perkuhn², Jassin Petersen¹¹, Julian Pietralla¹¹, Tina Sanders³, Anna Saupe¹¹, Johanna Schmidt¹¹, Mischa Schönke¹, Thekla-Regine Schramm³, Linting Sun⁹, Xu Sun^{9,14}, Dehao Tang^{12,13}, Jianhui Tang^{9,15}, Shichao Tian², Chen Tu^{9,1}, Fengping Wang^{7,8}, Xinming Wang¹⁶, Maike Wilschnack¹, Andreas Wittmann³, Zhen Xia^{12,13}, Kuanxu Xiong⁹, Jie Yang¹⁰, Ruifeng Zhang⁷, Xinning Zhang⁹, Zhaoru Zhang⁷, Xiaomei Zhen^{9,14,16}, Yisen Zhong⁷, Lei Zhou⁷, Meng Zhou⁷, Qian Zhou^{9,1}, Yiwu Zhu⁷

Author addresses:

¹ Leibniz Institute for Baltic Sea Research Warnemünde, Seestraße 15, 18119 Rostock, Germany

² Institute of Geology, University of Hamburg, Bundesstraße 55, 20146 Hamburg, Germany

³ Institute of Coastal Research, Helmholtz-Zentrum Geesthacht Centre for Materials and Coastal Research, Max-Planck-Straße 1, 21502 Geesthacht, Germany

⁴ Institute of Oceanography, University of Hamburg, Bundesstr. 53, 20146 Hamburg, Germany

⁵ Department of Aquatic Sciences and Assessment, Swedish University of Agricultural Sciences, Lennart Hjelm's väg 9, 75651 Uppsala, Sweden

⁶ Federal Maritime and Hydrographic Agency (BSH), Bernhard-Nocht-Straße 78, 20359 Hamburg, Germany

- ⁷ School of Oceanography, Shanghai Jiao Tong University, No. 1954 Huashan Road, Shanghai 200030, PR China
- ⁸ State Key Laboratory of Microbial Metabolism, School of Life Sciences and Biotechnology, Shanghai Jiao Tong University, Shanghai 200240, PR China
- ⁹ CAS Key Laboratory of Coastal Environmental Processes and Ecological Remediation, Yantai Institute of Coastal Zone Research, Chinese Academy of Sciences (YIC-CAS), 17 Chunhui Road, Yantai 264003, PR China
- ¹⁰ CAS Key Laboratory of Soil Pollution and Pollution Remediation, Institute of Soil Science, Chinese Academy of Sciences, 71 East Beijing Road, Nanjing 210008, PR China,
- ¹¹ Institute of Geology and Mineralogy, University of Cologne, Zùlpicher Str. 49a, 50674 Cologne, Germany
- ¹² Guangzhou Marine Geological Survey, No. 188 Guanghai Road, Guangzhou 510075, PR China
- ¹³ Southern Marine Science and Engineering Guangdong Laboratory, 1119 Haibin Road, Guangzhou 511458, PR China
- ¹⁴ University of Chinese Academy of Sciences, Beijing 100049, PR China
- ¹⁵ Center for Ocean Mega-Science, Chinese Academy of Sciences, Qingdao 266071, PR China
- ¹⁶ State Key Laboratory of Organic Geochemistry, Guangzhou Institute of Geochemistry, Chinese Academy of Sciences, 511 Kehua Street, Guangzhou 510640, PR China

Table of Content

Kurzfassung	7
Summary	9
1 Preface	11
2 Physical forcing and the pattern of emerging pollutants in South China Sea	14
2.1 Surface Kuroshio Intrusion into the South China Sea derived from Satellite Geostrophic Streamlines (Yisen Zhong, Meng Zhou, Joanna J. Waniek, Lei Zhou and Zhaoru Zhang)	14
2.2 Statistical characteristics of mesoscale eddies on the continental slope in the northern South China Sea (Meng Zhou, Zi Cheng, Yisen Zhong and Zhaoru Zhang)	15
2.3 Numerical simulation of Mangkhut typhoon waves in South China Sea (Mengxi Hu and Yisen Zhong)	17
2.4 Ecosystem production response to typhoon in the oligotrophic South China Sea (Yonghui Gao, Ji Li, Yisen Zhong, Meng Zhou and Joanna J. Waniek)	19
2.5 Holocene paleoenvironmental reconstruction of the inner South China Sea shelf near the Pearl River Delta based on geochemical and hydroacoustic investigations (Mischa Schönke, Olaf Dellwig, Jérôme Kaiser, Pingyuan Li and Helge W. Arz)	22
2.6 Sedimentary environmental evolution for the past 30 ka on the northern continental slope of the South China Sea (Pingyuan Li, Jianfei Lu, Zhen Xia and Huayang Gan)	24
2.7 Accumulation of recalcitrant organic matter in porewaters in sediment cores of the northern South China Sea (Yunru Chen and Fengping Wang)	26
2.8 The nitrogen cycle in the northern South China Sea: Impact of the Pearl River (Jan Maier, Carolin Perkuhn, Shichao Tian, Joanna J. Waniek, Niko Lahajnar, Kay Emeis and Birgit Gaye)	27
2.9 Estrogenic compounds in the Pearl River Estuary and coastal South China Sea (Carina Deich, Marion Kanwischer, Helena C. Frazão, Jana-Sophie Appelt, Ruifeng Zhang, Wenguo Li, Thomas Pohlmann and Joanna J. Waniek)	29
2.10 Distribution patterns of organic pollutants in water and sediment samples of the South China Sea (Kathrin Fisch, Ines Hand, Maike Wilschnack and Detlef E. Schulz-Bull)	31
2.11 Environment evolution and ecological impact of oxygen-depleted waters in the Pearl River Estuary and coastal area, China (Dehao Tang, Yugen Ni, Gaowen He and Zhen Xia)	32
2.12 Benthic foraminifera as bioindicators off the Pearl River Estuary (South China Sea): baseline study and potential application (Jassin Petersen, Julian Pietralla, Tamara Hechemer, Johanna Schmidt, Anna Saupe and Patrick Grunert)	34

2.13	Vertical Distribution and Size Structure of Zooplankton in Different Water Column in the Northern South China Sea (Kaixuan Chen, Meng Zhou, Joanna J. Waniek, Yisen Zhong and Yiwu Zhu)	35
3	Investigations of pollutants dispersal in the Bohai and Yellow Sea	38
3.1	Numerical simulation of pollution's transportation on the East Chinese Shelf and in the northern South China Sea (Wenguo Li, Bernhard Mayer and Thomas Pohlmann)	38
3.2	The budget of nitrate isotopes in Bohai Sea based on an isotopic balance model (Shichao Tian, Birgit Gaye, Jianhui Tang, Yongming Luo, Tina Sanders, Kirstin Dähnke and Kay-Christian Emeis)	40
3.3	Environmental occurrence and distribution of selected current-used pesticides in the Chinese Bohai Sea and surrounding Rivers (Célia P.M. Bento, Tanja Naumann, Andreas Wittmann, Jianhui Tang, Xiaomei Zhen and Ralf Ebinghaus)	42
3.4	Halogenated flame retardants in the sediments of the Chinese Yellow Sea and East China Sea (Yanan Li and Jianhui Tang)	43
3.5	Legacy and novel halogenated flame retardants in seawater and atmosphere of the Bohai Sea, China (Lin Liu, Xiaomei Zhen, Xinming Wang, Yanfang Li, Xu Sun and Jianhui Tang)	44
3.6	Identification of elements distribution patterns in the delta-estuary region by a combined magnetic and isotopic approach (Yuan Li and Yongming Luo)	45
4	Comparison of the European and Asian marginal seas	48
4.1	Occurrence and risk of organic UV absorbers in marine sediments of Europe and China (Andreas Wittmann, Christina Apel, Jianhui Tang and Ralf Ebinghaus)	48
4.2	Emerging and novel per- and polyfluoroalkyl substances in Chinese and German river water impacted by point sources (Hanna Joerss, Jianhui Tang, Thekla-Regine Schramm, Linting Sun, Chao Guo, Frank Menger, Lutz Ahrens and Ralf Ebinghaus)	49
4.3	Spatial distribution of microplastics: comparison between the Bohai and Baltic seas (Qian Zhou, Chuancheng Fu, Jie Yang, Kuanxu Xiong, Yuan Li, Chen Tu, Lianzhen Li, Yongming Luo and Joanna J. Waniek)	51
4.4	Characterization of biofilms formed on the surface of diverse types of microplastics in the seawater of the Baltic Sea (Chen Tu, Qian Zhou, Ying Liu, Xinning Zhang, Joanna J. Waniek and Yongming Luo)	52
5	Conclusions and outlook	54
	Acknowledgements	54
	References	55

Kurzfassung

Das deutsch-chinesische Verbundvorhaben Megacity's fingerprint in Chinese marginal seas: Investigation of pollutant fingerprints and dispersal (MEGAPOL) geht nach drei Jahren intensiver Zusammenarbeit (01.08.2017-31.07.2020; verlängert bis 31.12.2020) zu Ende. MEGAPOL hatte zwei regionale Schwerpunkte. Der eine konzentrierte sich auf den Mündungsbereich des Perlfusses im Südchinesischen Meer und der andere auf das Gelbe Meer mit dem Yangtse Fluss sowie auf die Bohai See mit dem Gelben Fluss. Die Verbundpartner auf deutscher Seite sind das Leibniz-Institut für Ostseeforschung Warnemünde, das Institut für Geologie und das Institut für Meereskunde der Universität Hamburg, sowie das Institut für Küstenforschung des Helmholtz Zentrums Geesthacht. Auf chinesischer Seite sind die Verbundpartner der Guangzhou Marine Geological Survey, die School of Oceanography der Shanghai Jiao Tong Universität, das Second Institute of Oceanography SOA, Hangzhou, das National Marine Environmental Monitoring Centre, SOA, Dalian und das Yantai Institute of Coastal Zone Research, CAS, Yantai. Die Prozessstudien wurden von Deutschland durch das BMBF (03Fo786A/B/C) im Rahmen der Wissenschaftlich-Technischen Zusammenarbeit (WTZ) mit China finanziert sowie von China durch die State Ocean Organisation (SOA).

Der Verbund hatte zum Ziel, die Umweltveränderungen in den genannten Schelfregionen und den Randmeeren zu untersuchen und damit die Folgen der Entstehung von Megastädten für das marine Ökosystem abzuschätzen. Die Untersuchungsgebiete stellen ideale Modellsysteme dar, um Austauschprozesse zwischen Land und Ozean, Veränderungen der physikalischen Antriebe (Monsun, Zirkulation), anthropogene Stoffflüsse (u.a. Mikroplastik, Schadstoffe) und somit die Effekte von Ballungszentren auf die Wechselwirkung Land-Küste-Ozean sowie die Auswirkungen von klimatischen Änderungen in sensiblen marinen Ökosystemen besser zu verstehen. Die Probennahme im Südchinesischen Meer wurde auf drei mehrwöchigen Expeditionen mit chinesischen Forschungsschiffen (HAI YANG DI ZHI SHI HAO 2015, HAI YANG DI ZHI SHI HAO 2018) und dem deutschen Forschungsschiff SONNE (2019) durchgeführt. Die Beprobung in der Bohai See und im Gelben Meer fand im April und August 2018 mit dem chinesischen Forschungsschiff R/V DONG FANG HONG 2 statt. Flussproben wurden im Mai und Juli bis November im Gelben Fluss genommen sowie im November aus dem Daliao, Hai, Luan und Xiaoqing Fluss. Für beide regionalen Schwerpunkte lieferten die physikalischen, bio-geochemischen und ökosystemaren Modellierungen zusätzliche Erkenntnisse zum Einfluss von wechselnden Umweltparametern auf die marinen Stoffkreisläufe (N, P, C) und ermöglichten Aussagen zu der zeitlichen und räumlichen Variabilität der ozeanischen Prozesse.

Der MEGAPOL Verbund wurde durch die Aktivitäten des BMBF Verbundes Südchinesisches Meer-Natürliches Laboratorium unter klimatischen und anthropogenen Stress (FKZ 03Go269A-B, SOCLIS) erweitert, in dessen Rahmen die Expedition mit dem deutschen Forschungsschiff SONNE (SO269) im August 2019 im Untersuchungsgebiet am nördlichen Schelfrand des Südchinesischen Meeres im Mündungsbereich des Perlfusses stattfand. Auf der Expedition wurde u.a. eine Verankerung für einen Zeitraum von 2 Jahren am nördlichen

Kontinentalhang des Südchinesischen Meeres ausgesetzt, wodurch die wissenschaftlichen Fragestellungen und die Infrastruktur von MEGAPOL erweitert wurden. Diese Arbeiten wurden durch das TRAN Projekt (Zeitliche Muster anthropogener und natürlicher Partikel am Kontinentalhang des Südchinesischen Meeres, FKZ 01DO17038) auf der deutschen Seite finanziert.

In diesem Bericht fassen wir die ersten Ergebnisse der Untersuchungen in Form erweiterter Kurzbeschreibungen deutscher und chinesischer KollegInnen zusammen, die in einer Online-Konferenz am 28. und 29. Oktober 2020 vorgestellt wurden.

Summary

The bilateral Sino-German joint project Megacity's fingerprint in Chinese marginal seas: Investigation of pollutant fingerprints and dispersal (MEGAPOL) comes to an end after three years of intensive cooperation (01.08.2017-31.07.2020; extended until 31.12.2020). MEGAPOL had two regional focuses, one at the mouth of the Pearl River in the South China Sea and one on the Yellow Sea with the Yangtse River and on the Bohai Sea with the Yellow River.

The Leibniz Institute for Baltic Sea Research Warnemünde, the Institute of Geology and the Institute of Oceanography of the University of Hamburg, the Institute for Coastal Research of the Helmholtz Centre Geesthacht from Germany and the Guangzhou Marine Geological Survey, the School of Oceanography of the Shanghai Jiao Tong University, the Second Institute of Oceanography SOA, Hangzhou, the National Marine Environmental Monitoring Centre, SOA, Dalian and the Yantai Institute of Coastal Zone Research, CAS, Yantai from China cooperated in this network. The process studies were financed on the German side by the BMBF (03F0786A/B/C) within the framework of the WTZ China Initiative, whereas the State Oceanic Administration (SOA) financed the studies on the Chinese side.

The aim of the network was to investigate environmental changes in the aforementioned marginal seas and their shelf areas in order to understand the effects of anthropogenic and natural changes, as a consequence of the formation and development of megacities, on the marine ecosystem. The study areas represented an ideal model system to better understand land-ocean exchange processes, changes in physical drives (monsoon, circulation), anthropogenic matter fluxes (including microplastics, pollutants), the effects of urban agglomerations on the land-coast-ocean interaction, and the effects of climatic changes in a very sensitive marine ecosystem. Sampling was carried out on three expeditions lasting several weeks on Chinese research vessels (HAI YANG DI ZHI SHI HAO 2015, HAI YANG DI ZHI SHI HAO 2018) and the German research vessel SONNE (2019) in the South China Sea. Sampling in the Bohai and Yellow Sea was carried out in April and August 2018 by the research vessel R/V DONG FANG HONG 2. River samples were taken in May, July to November from the Yellow River, and in November from Daliao River, Hai River, Luan River and Xiaoqing River. For both regional foci, physical, bio-geochemical and ecosystem modelling provided additional insights into the influence of varying environmental parameters on changes in biogeochemical cycles of elements (N, P, C) and allowed the assessment of the temporal and spatial variability of oceanic processes.

The MEGAPOL consortium was expanded by the activities of the BMBF project South China Sea Natural Laboratory under Climatic and Anthropogenic Stress (FKZ 03G0269A-B, SOCLIS). The central activity in SOCLIS was the expedition with the German research vessel SONNE (SO269) in August 2019 in the working area at the northern shelf edge of the South China Sea in the research area of the Pearl River. During the expedition, among other things, a mooring was deployed for a period of 2 years on the northern continental slope of the South China Sea, thus expanding the scientific questions and infrastructure of MEGAPOL. This work was

financed by the TRAN project (Temporal Patterns of Anthropogenic and Natural Particles on the Continental Slope of the South China Sea, FKZ 01DO17038) on the German side.

In this report we summarize the first results of the investigations in the form of extended short descriptions presented by German and Chinese colleagues, which were presented in an online conference on 28 and 29 October 2020.

1 Preface

Worldwide, shelf areas are the most productive regions in the world ocean but represent only 7% of the ocean surface and less than 0.5% of the ocean volume. Their proximity to the land masses makes them particularly important for understanding the exchange processes between coastal regions and the open ocean, in terms of energy and mass transfer, control of anthropogenic and terrestrial fluxes, transport, distribution and deposition of pollutants, and primary production. Shelf seas react rapidly to environmental changes on different time and space scales as their carbon turnover rates are only a few days to weeks. The amount of organic material reaching the seafloor and being buried in sediments is higher in shelf areas compared to the open ocean. Shelf seas are, therefore hotspots of chemical degradation processes as well as redox reactions in the sediments (e.g. denitrification, reduction of trace metals) strongly impacting the C, N, P and Fe cycles. In this context, the pollutants introduced are of importance, which have an adverse effect on the ecosystem. The consequences of climate change on the one hand and anthropogenic influences on the other hand are only fragmentarily known in the coastal ocean. In the recent past, large metropolitan areas have emerged along the coasts (SEITZINGER et al. 2012, UNESCO 2016), which have drawn on the resources of the hinterland and catchment areas and are exerting steadily increasing pressure on the coastal environment due to the industrialization of the regions. In 1970 the United Nations identified three megacities, the number rose to 10 by 1990 and 28 in 2014, with prediction of 40 megacities world wide by 2030. Many of those being located in the worlds least developed or threshold countries.

The development of coastal megacities on the Asian continent, especially in China with a simultaneous industrialization of the hinterland, is omnipresent (UNESCO 2016). However, the consequences for the marginal seas of these anthropogenic interventions are only rudimentarily understood and studied, especially with regard to eutrophication and modern/emerging pollutants (microplastics, hormones, drugs).

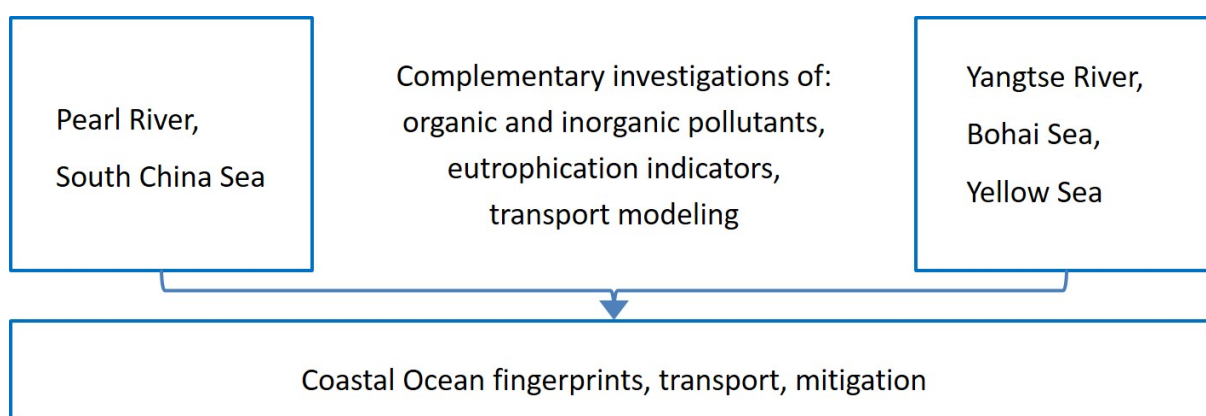


Fig. 1: Structure and regional foci of the Sino-German MEGAPOL Project.

The great social and economic relevance of the coastal regions and the marginal seas worldwide were the scientific rationale for the Sino-German project MEGAPOL (Fig. 1), which aimed to answer the following questions:

- Are the different climatic conditions, geology of the catchment areas, agricultural and industrial use of the land reflected in regionally specific distributions of substances introduced and deposited in China's marginal seas (South China Sea vs. Bohai Sea and Yellow Sea)?
- To what extent is the "fingerprint" of the megacities in marginal seas mapped and/or modified by the prevailing hydrographic conditions: open shelf and circulation in the South China Sea versus restricted exchange and circulation in the Bohai Sea and the Yellow Sea?
- What is the function of the sediments in these regions with respect to anthropogenic pressure, in particular the introduced modern pollutants (e.g. microplastics, UV filters, drug residues)?

The Bohai Sea and the Yellow Sea as well as the East China Sea in the south are shallow marginal seas of the Northwest Pacific. They lie almost entirely on the north-eastern Asian shelf. While the Yellow Sea and the East China Sea are characterized by a strong exchange with the Pacific Ocean due to their open seaward boundary, the Bohai Sea is a relatively closed sea, which has only a limited exchange with the open ocean via the 100 km wide Bohai Strait. Ocean currents throughout the region are dominated by the alternation of summer and winter monsoons throughout the region. The effect of these seasonal changes including strong seasonal variations of water and nutrient supply are augmented by the shallow water depth of less than 50 m in large parts of these marginal seas leading to significant ecosystem changes. During the last decades, river discharges have decreased significantly, resulting in increased salinity and decreased phosphate and silicate inputs. At the same time, the input of reactive nitrogen from wastewater and fertilizers has increased tenfold (NING et al. 2010, ZHANG et al. 2004, ZHAO et al. 2002). Strong eutrophication, particularly in the area of the river plumes of the Yellow River and the Yangtze, is the consequence, which seasonally leads to the formation of so-called oxygen-free death zones (CHEN et al. 2014). Nutrient inputs will further increase with the planned Bohai Rim Urban Agglomeration/ Northern Yellow Sea and thus further promote eutrophication and oxygen depletion. The South China Sea (SCS) is the largest marginal sea of the Pacific Ocean with a well-developed shelf in the north. The northern shelf of the South China Sea, its transitional region to the continental slope, and the deep SCS are highly dynamic regions influenced by seasonally and inter-annually varying forces; their effects are modified and amplified by climatic changes caused by both, natural and anthropogenic processes. The SCS itself is oligotrophic, whereas the northern shelf is eutrophic and occasionally suffers from anoxia due to the decay of biomass from locally enhanced productivity.

The selected marginal seas offer a unique opportunity to investigate the impact of climatic and anthropogenic pressures on the marine ecosystem, as their distinct shelf areas play a key function in the land-ocean interaction. According to the 2007 IPCC report, Southeast Asia and the South China Sea will also experience a temperature increase of up to 6 °C by 2100. This temperature rise will be accompanied by increased precipitation and extreme weather conditions, with obvious consequences for the land, the people living there and the marine ecosystems.

During our MEGAPOL online general assembly on 28 and 29 October 2020 a number of studies were presented grouped into different topics. The sessions on day one were dedicated to the South China Sea and covered physical oceanography, marine chemistry, marine geology and biological oceanography. ZHONG et al. presented their work on Kuroshio Current intrusions, whereas CHENG et al. looked at mesoscale eddies in the region. The typhoon Mangkhut which also affected one of our cruises was simulated by HU and ZHONG, and its impact on the environmental conditions was presented by GAO et al. Holocene sediments, sediment evolution over 30 ka and accumulation of recalcitrant organic matter were presented by SCHÖNKE et al., LI et al. and CHEN and WANG, respectively. In the following talks pollution aspects (FISCH et al., DEICH et al.), nitrogen cycle (MEIER et al.), oxygen deficiency (TANG et al.), benthic foraminifera as bioindicators of environmental change (PETERSEN et al.) and research on the trophic structure of the South China Sea (CHEN et al.) were presented.

The focus on the second day was on the East China Sea and the Yellow Sea, modelling efforts as well as a comparison of specific ecosystems to the Baltic Sea. First, the modelling results were presented by LI et al. for the East Chinese Shelf and the South China Sea, followed by the nitrate budget of the Bohai Sea (TIAN et al.). The next group of presentations dealt with different groups of pollutants, e.g. glyphosate and AMPA (BENTO et al.), Neonicotinoids and their metabolites (NAUMANN et al.), halogenated flame retardants (LI et al.), their legacy and new species (LIU et al.). LI et al. used a combination of the magnetic and the isotopic approaches to understand the distribution of elements in a delta-estuary system. In the next talk UV absorbers (per- and polyfluoroalkyl substances) found in sediments were studied (WITTMANN et al.). The session closed with two talks about microplastics distribution patterns (ZHOU et al.) and biofilm formation (TU et al.).

Joanna J. Waniek¹, Detlef E. Schulz-Bull¹, Birgit Gaye², Ralf Ebinghaus³, Friederike Kunz¹, Thomas Pohlmann⁴, Kay-Christian Emeis^{2,3}

2 Physical forcing and the pattern of emerging pollutants in South China Sea

In this chapter the South China Sea, especially the northern shelf and the Pearl River, is in focus as it provides a unique opportunity to understand the impact of climatic and anthropogenic pressures on the marine ecosystem. Its distinct shelf areas are a key feature in the land-ocean interaction. According to the 2007 IPCC report, Southeast Asia and the South China Sea will also experience a temperature increase of up to 6°C by 2100. This temperature increase will be accompanied by increased precipitation and extreme weather (e.g. typhoons), with obvious consequences for the land, the people living there, and the marine ecosystems. One part of the investigations in the MEGAPOL project has therefore the regional focus on the northern shelf of the South China Sea and thematically on the study of the distribution patterns of selected anthropogenic pollutants. It is aiming at identifying their sources and sinks, determining turnover rates, and describing the "fate" of the investigated pollutants. Of particular interest to us are emerging pollutants (microplastics, pharmaceuticals, UV filters), heavy metals, and eutrophication, all closely linked to anthropogenic pressures, which we examine in light of the physical driving forces (e.g., monsoon), processes (transport, dispersion) and events like typhoons.

2.1 Surface Kuroshio Intrusion into the South China Sea derived from Satellite Geostrophic Streamlines (Yisen Zhong⁷, Meng Zhou⁷, Joanna J. Waniek¹, Lei Zhou⁷ and Zhaoru Zhang⁷)

The Kuroshio intrusion into the Luzon Strait plays a very important role in the mass and heat exchange between Pacific Ocean and South China Sea (SCS). Due to the paucity of observational data, there still exists a debate on describing the characteristics of intrusion and interpreting its mechanism at various time scales. In this study, using geostrophic streamlines derived from 1993–2018 daily satellite altimeter data, we propose a new method to recognize the flow pattern of Kuroshio intrusion into South China Sea by tracking the extension of each streamline originated from Kuroshio. The streamlines are categorized into three traditional types: leaping across the strait, loop current and direct intrusion into SCS. The flow pattern can be any combination of these three kinds. This streamline-based method represents a more elaborate classification and therefore provides new insights into the Kuroshio intrusion mechanism at different time scales.

Table 1: The occurrence frequency of each possible combination of streamlines over the entire period, in December and June. Note the sum of each column may be not equal to 1 due to a small number of unclassified streamlines.

Streamline type	Frequency	Frequency in Dec	Frequency in Jun
Leap	48.2%	9.7%	89.5%
Leap+Loop	17.4%	18.2%	6.8%
Leap+Intrude	9.8%	24.4%	0%
Leap+Loop+Intrude	22.9%	47.6%	1.3%

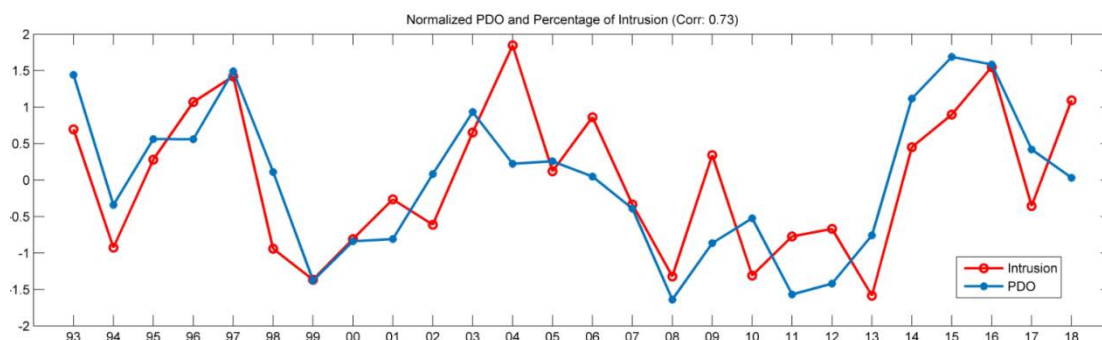


Fig. 2: Interannual Pacific Decadal Oscillation index (blue) and percentage of intrusion streamlines (red). Both of them are normalized. The correlation coefficient between them is 0.7.

The streamline analysis shows that the Kuroshio consists of all the three kinds of streamlines over 22% days of this period (Table 1). The intrusion streamlines account for 20% of the total in winter but almost all the streamlines leap across the strait in summer. Most of the intrusion streamlines enter the Luzon Strait via the deep channel south of Babuyan Island, while the leaping streamlines go into the strait mainly through Balintang Channel and subsequently out of the strait through Bashi Channel. At the seasonal scale the intrusion streamlines are mostly located in the left part of the Kuroshio with cyclonic velocity shear, which means the seasonal variation of the intrusion is merely the seasonality of these streamlines. On an interannual time scale, the percentage of intrusion streamlines show a strong correlation with ENSO and PDO indices. The correlation coefficient is over 0.7, much higher than that in previous studies (usually lower than 0.6), suggesting this new method can better capture the interannual variation of Kuroshio intrusion (Fig. 2). Nearly all the intrusion streamlines fail to track back upstream to the North Equatorial Current (NEC), since they are located too close to the coast where the accuracy of satellite data may be very poor. However, the analysis of leaping streamlines reveals that the NEC bifurcation latitude has a larger variation than that in preceding numerical studies. During El Niño years, the bifurcation latitude reaches the northmost around 15°N, and both the width of Kuroshio Current and the Kuroshio transport increase. The bifurcation latitude stays south of 14°N with decreased current width and transport during La Niña years.

Acknowledgements:

This research is supported by the National Natural Science Funding of China (Grant #: 41706014) and Sino-German cooperation in ocean and polar research – Megacity's fingerprint in Chinese marginal seas: Pollutant fingerprints and dispersal transformation.

2.2 Statistical characteristics of mesoscale eddies on the continental slope in the northern South China Sea (Meng Zhou⁷, Zi Cheng⁷, Yisen Zhong⁷ and Zhaoru Zhang⁷)

The South China Sea (SCS) is considered as oligotrophic where productivity is limited by dissolved iron and other macronutrients. However, there is an active mesopelagic ecosystem with high biomass of 30 g m⁻² in the SCS. Studies found that even though the biomass of

primary producers is very lower, the primary production is high approximately $300 \text{ mg C m}^{-2} \text{ d}^{-1}$. For understanding mechanisms to support the primary production and food demand of mesopelagic fish, the role of mesoscale eddies in cross-slope transport of nutrients and biomass in the northern continental slope region are studied based on satellite altimetry data from 1993 to 2016. The results reveal that a total of 147 eddies including 70 cyclonic eddies (CEs) and 77 anticyclonic eddies (ACEs) are detected in the continental slope region (CSR). The eddies are mainly originated from two areas: near the Dongsha Islands (DS) and southwest of Taiwan (SWT), which contribute more than 60% of the total (Fig. 3a, b).

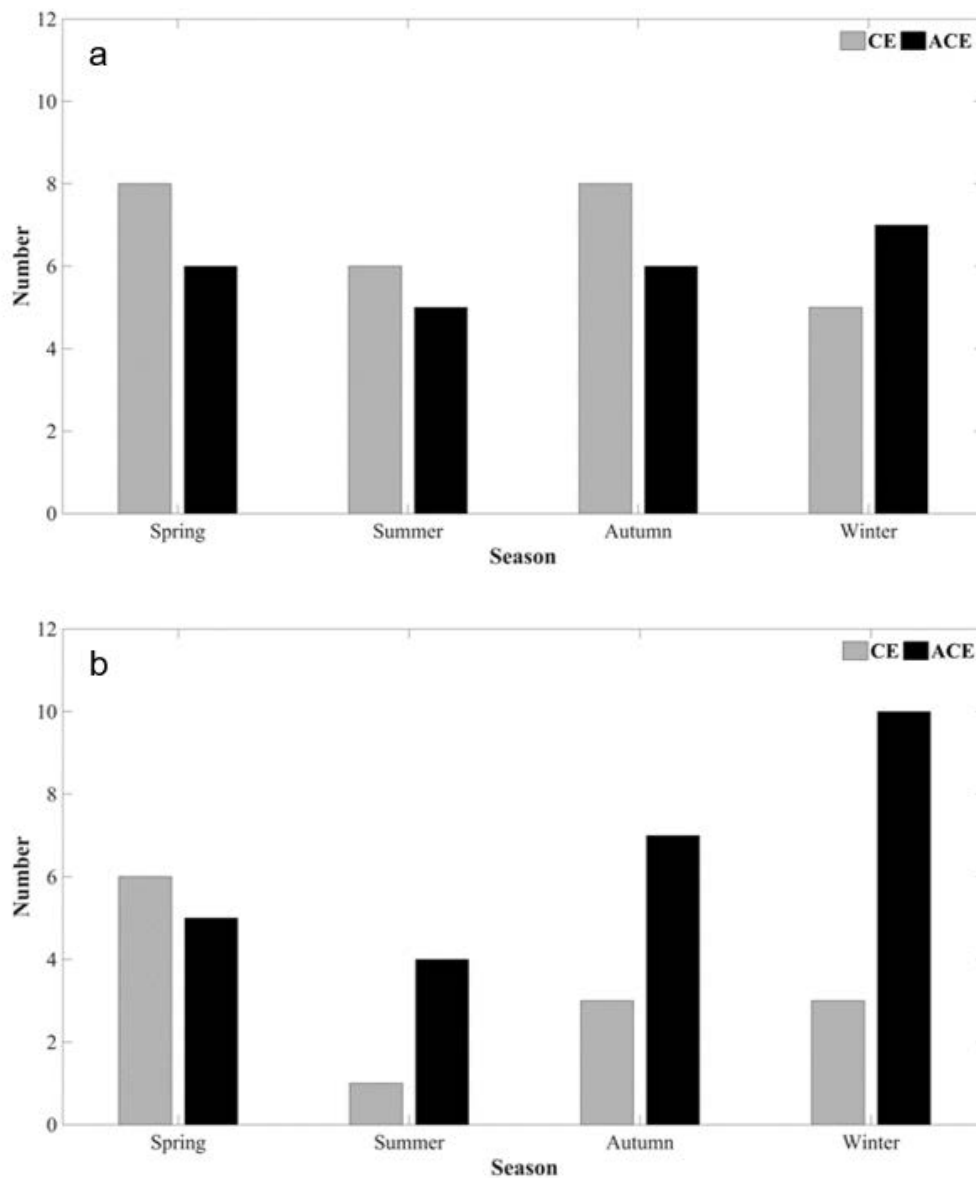


Fig. 3: Seasonal distributions of the number of eddies that are generated in the DS (a) and in the SWT (b) and subsequently enter the CSR.

According to the spatial distribution of eddy relative vorticity, both cyclonic and anticyclonic eddies generally weaken as they propagate westward roughly along the slope isobaths. During the life span of eddies, the ACEs move slightly faster along the isobaths, while the CEs tend to cross the isobaths into the shallow water or deep basin (Fig. 4a–d). After leaving the

CSR, the ACEs generally move further into the basin areas, and the CE's still linger around the CSR. The eddy propagation on the continental slope is found to be linked with the mean flow field to some degree since the eddy trajectories have noticeable seasonal cycles in agreement with the seasonality of geostrophic current, which indicates that the eddy propagation velocity is largely determined by the along-slope geostrophic current in both magnitude and direction.

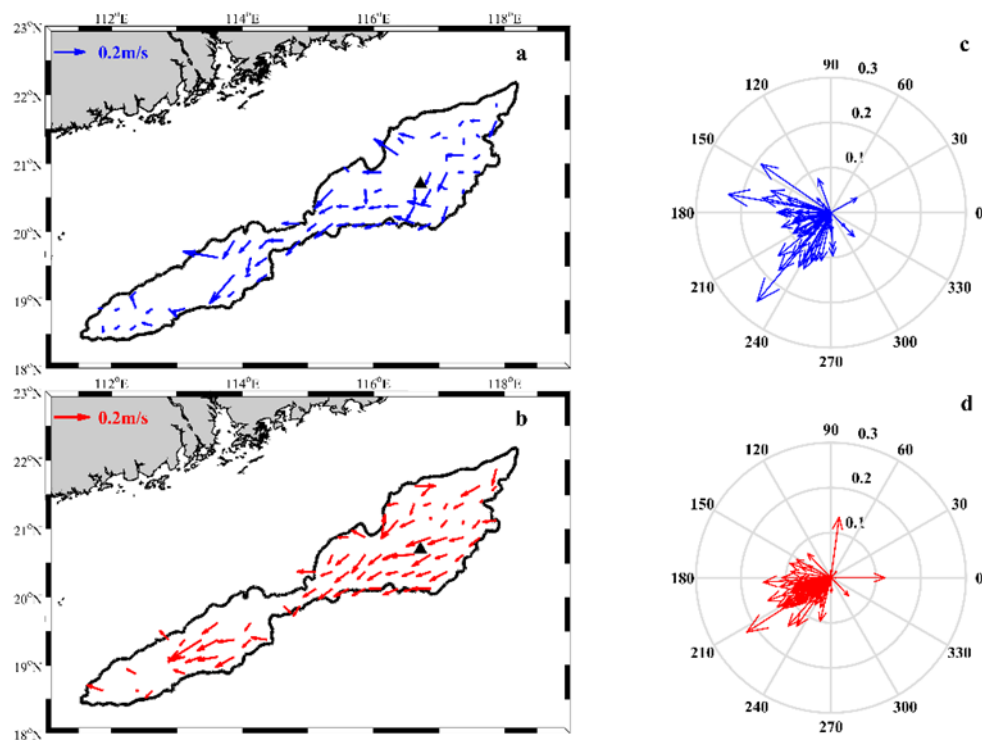


Fig. 4: Mean eddy propagation velocities in the CSR. a and b are eddy velocity fields of CEs and ACEs, respectively; c and d are compass diagrams of CE and ACE propagation velocities, respectively.

Acknowledgements:

This research is supported by the National 973 Program on Key Basic Research (Grant # 2014CB441500), the National Natural Science Funding of China (Grant #: 41706014) and Sino-German cooperation in ocean and polar research - Megacity's fingerprint in Chinese marginal seas: Pollutant fingerprints and dispersal transformation.

2.3 Numerical simulation of Mangkhut typhoon waves in South China Sea (Mengxi Hu¹² and Yisen Zhong⁷)

The tropical cyclones as the most extreme meteorological events can generate complex and disastrous ocean waves propagating towards the shorelines, which may cause vast economic losses and human casualties in the South China Sea. It is thus of great importance and interest both practically and scientifically to model the typhoon waves and help understand their physical properties (Komen et al. 1994, Xu et al. 2017, Young 2006).

A third-generation wave model is driven by the synthetic wind field combined with the Holland wind and the surface wind product from National Centers for Environmental Prediction (NCEP), in order to numerically simulate the TWs generated by the 22nd typhoon "Mangkhut" in 2018. The modelled results are in good agreement with the buoy-based observations (Fig. 5a–f). Therefore, the model can well simulate the typhoon waves under "Mangkhut" in South China sea.

The temporal and spatial characteristics of the wind-sea and swells during the typhoon were studied. The results show that the far field is dominated by swells radiating from intense wind region, and the maximum significant wave height is always located on the front-right side of the typhoon moving direction where wind-sea dominates (Fig. 6). This indicated that the typhoon waves have obvious asymmetry. Except for the left rear quadrant of the typhoon's forward direction, the corresponding dominated waves gradually change from wind-seas to swells as the distance from the typhoon center increases.

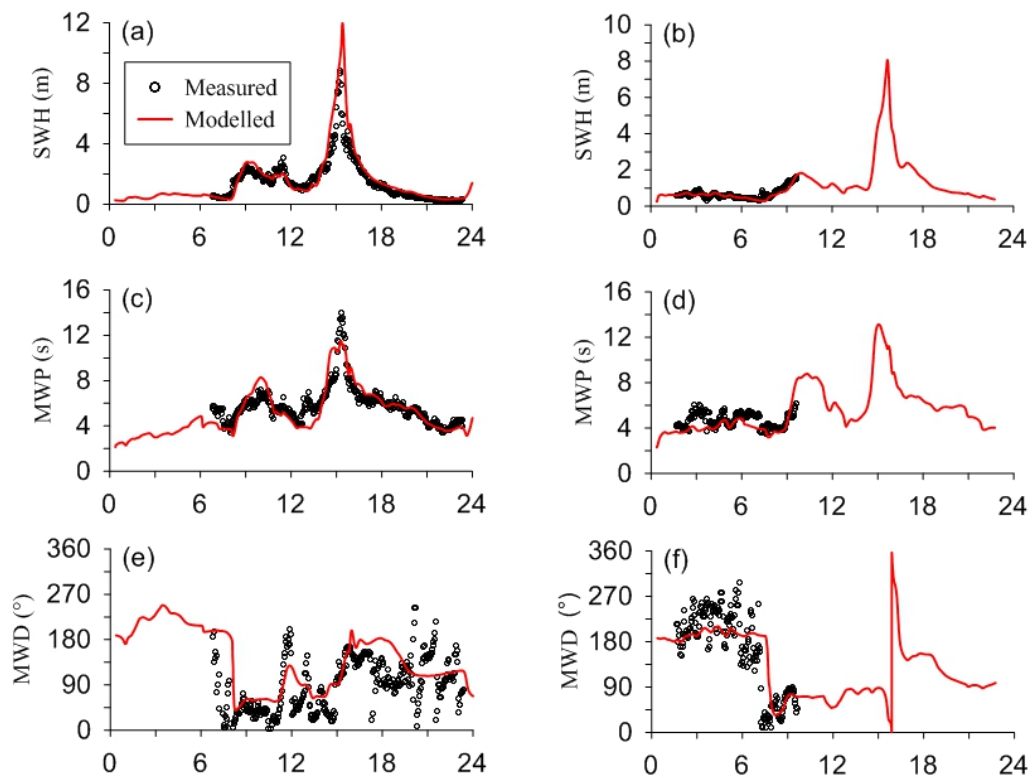


Fig. 5: Comparison of simulated and measured (a, b) significant wave height, (c, d) mean wave period, (e, f) mean wave direction. The left and right columns correspond to two different stations.

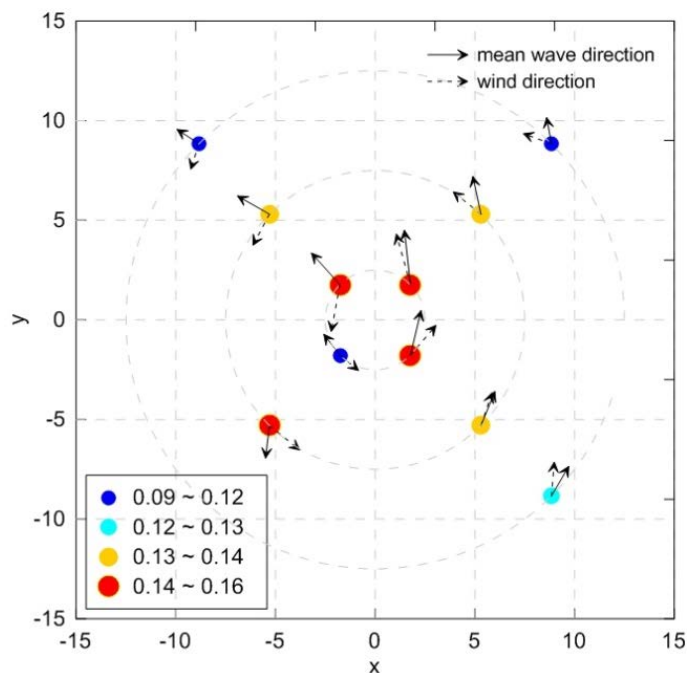


Fig. 6: The spatial distribution of the dimension free peak frequency ν . According to the fetch-limited theory, locations are dominated by wind-sea when $\nu > 0.13$, and vice versa, it is swell-controlled. The data is projected onto a frame with the typhoon's forward direction as 0° , and the typhoon center is the origin. The solid arrow indicates the relative wave direction, and the dashed arrow is the relative wind direction. The distance of the coordinate axis is based on the maximum wind speed radius.

Acknowledgements:

This work was funded by Project of China Geological Survey (CGS) (No. DD20190218) and Leibniz Institute for Baltic Sea Research Warnemünde. We thank the crews in Hai Yang Di Zhi ship for their great effort in wave buoys deployments on the No.201809 cruise.

2.4 Ecosystem production response to typhoon in the oligotrophic South China Sea (Yonghui Gao⁷, Ji Li⁷, Yisen Zhong⁷, Meng Zhou⁷ and Joanna J. Waniek¹)

Marine biological carbon fixation via phytoplankton photosynthesis converts atmospheric CO_2 to particle organic carbon (POC), which becomes major source of carbon export flux to the deep ocean. Although continental shelf only accounts for 7% of the world ocean area, they contribute near 1/3 of the oceanic CO_2 intake from atmosphere (MULLER-KARGER, 2005). As the largest continental shelf in Asia and Pacific Ocean, South China Sea (SCS) has drawn much attention in biological carbon intake.

Net community production (NCP), the deduction of ecosystem respiration from the biological carbon uptake, is valuable because it can accurately estimate the carbon sequestration in the ocean. Dissolved oxygen (DO)/argon (O_2/Ar) ratios in the oceanic mixed layer are indicative of net community production (NCP) because O_2 and Ar share similar physical solubility properties, but only O_2 is biologically produced or consumed (CASSAR et al. 2009). In this

study, we use the continuous O_2/Ar method to map the net community production thoroughly in the continental shelf of SCS before and after a typhoon (Fig. 7).

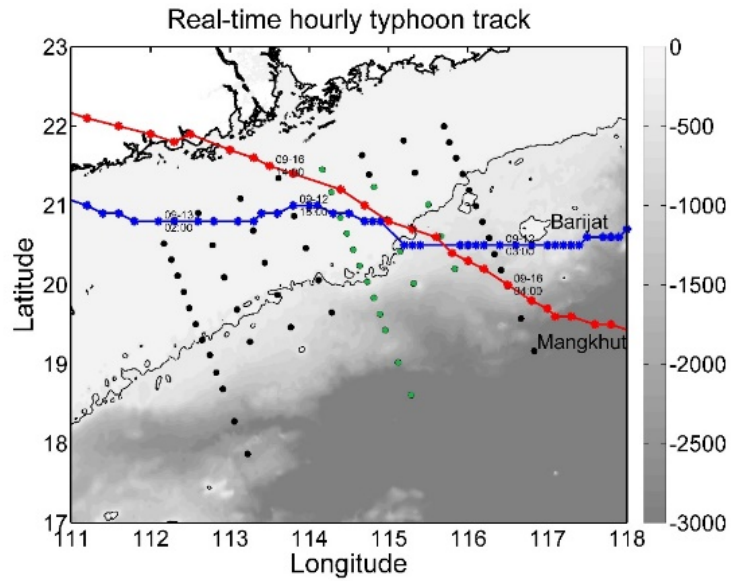


Fig. 7: Bi-typhoons, Barjat (blue line, Sept. 12-14) and Mangkhut (red line, Sept. 16-18), passed through the central research region twice. Dark and green dots indicate the CTD sampling stations before and after typhoon.

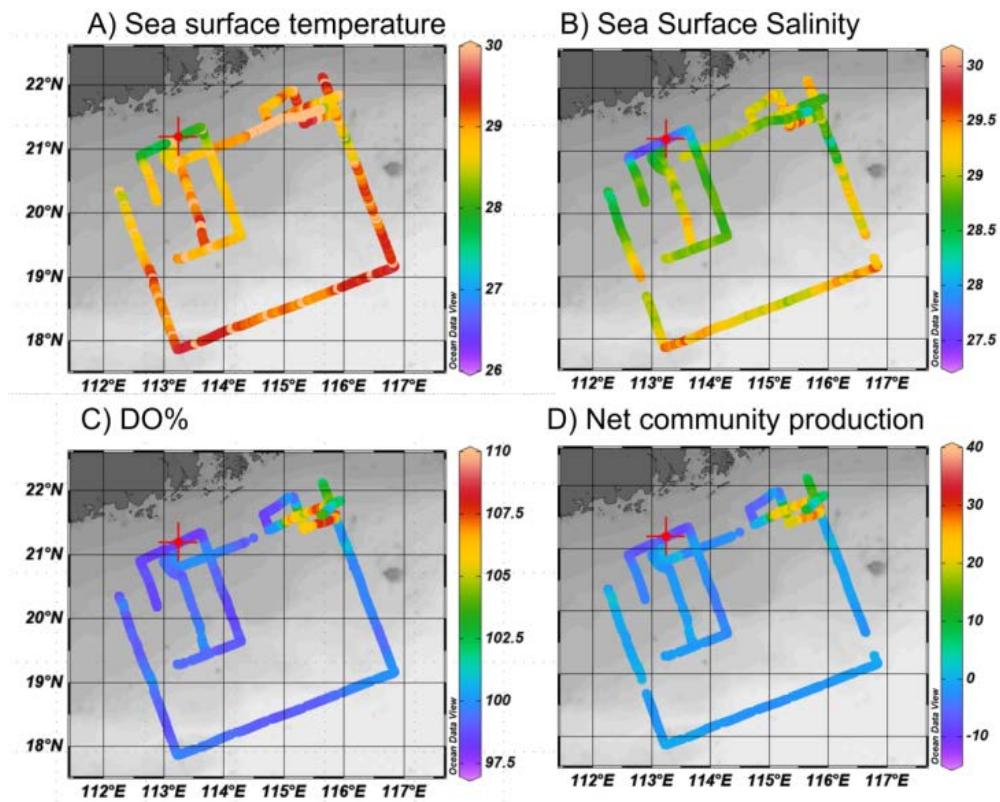


Fig. 8: Spatial distribution of sea surface temperature ($^{\circ}C$, A), Salinity (B), DO% (C) and Net community production ($mmol\ C\ m^{-2}\ d^{-1}$, D) before typhoons.

Before typhoon (Sept. 2–14, 2018), sea surface temperature changed consistently with salinity (Fig. 8), and both increased from nearshore to offshore region (Fig. 8A, B). NCP and DO% in most of water, especially in the offshore region, were slightly under-saturated (Fig. 8C, D). Summer monsoon, driven by the north-east wind, directly affect the surface circulation, thus SCS exhibit distinguished monsoon-driven pattern in the primary productivity and nutrient dynamics. DO% were positive and NCP were up to $33 \text{ mmol C m}^{-2} \text{ d}^{-1}$ in which upwelling and the Pear River plume might deliver nutrients and alleviate the nutrient limitation (Fig. 8C, D).

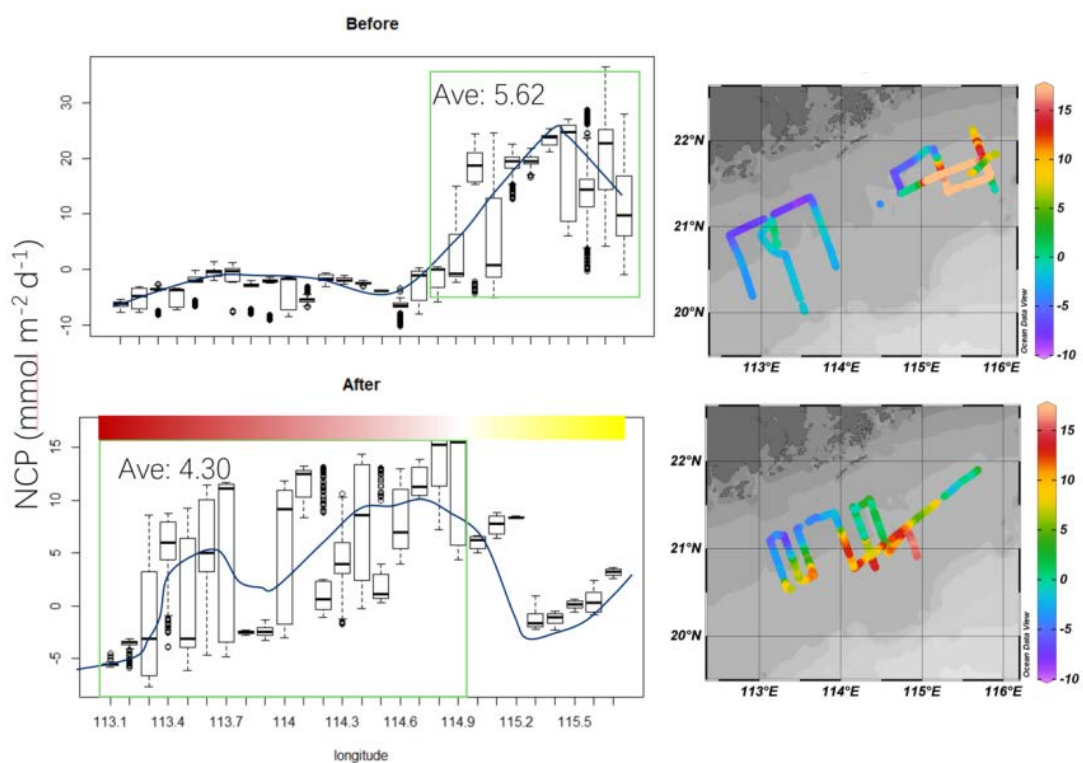


Fig. 9: Net community production (NCP) changes in response to typhoon. The line in the bars is the median value; the bottom and top edges of the box indicate the 25th and 75th percentiles; the lower and upper extent of the bars are the 10th and 90th percentiles; the dots are outliers.

Moreover, tropical cyclones (i.e., typhoons) occur frequently in summer. During our investigation (Sept. 1–30, 2018), typhoon Barjat and Mankhut passed through the central region in Sept. 11 and Sept. 16, respectively (Fig. 7). Typhoon-induced cooling, along with vertical mixing, entrainment, and upwelling, lead to transport of nutrient-rich deep water to the nutrient-depleted surface, thereby stimulated phytoplankton growth and induced an increase in NCP. Although autotrophic center changed due to strong mixing and dilution, ecosystem turned to autotrophic in most of the overlapped region before and after typhoon (Fig. 9). The overall contribution of typhoons to the NCP is around 30% in the overlapped study region in SCS. This study provide first underway estimation in production and would help to gain better understanding of the initiation of phytoplankton blooms in later summer and their impacts on the local biological carbon uptake.

2.5 Holocene paleoenvironmental reconstruction of the inner South China Sea shelf near the Pearl River Delta based on geochemical and hydroacoustic investigations (Mischa Schönke¹, Olaf Dellwig¹, Jérôme Kaiser¹, Pingyuan Li^{1,2} and Helge W. Arz¹)

Marginal Seas are highly productive and dynamic systems playing an important role for biogeochemical and pollutant exchange processes between the land and the ocean. The South China Sea (SCS) is one of the largest semi enclosed basins in the western Pacific Ocean and comprises both a broad shallow shelf in the northern part and a large NE–SW oriented abyssal basin in the center part. In the SCS, the Pearl River Delta (PRD) is one of the key regions to investigate the land-ocean interaction and has been studied extensively since the 1980s (TANG et al. 2010). The complex natural conditions of the PRD, including seasonal changes in longitudinal currents and high river runoff (LÜDMANN et al. 2001), in combination with the rapid and extreme high urbanization (Fig. 10) makes it a challenging task to study how natural and anthropogenically induced stress act on the marine environment. While most studies focus on the Quaternary deposits in the PRD (TANG et al. 2010, LIU et al. 2014), only few papers deal with the Holocene sedimentary conditions (TANG et al. 2010, LÜDMANN et al. 2001, WEI & WU, 2011).

However, a good understanding of recent sedimentation patterns and geochemical conditions is an essential step to differentiate and understand natural and anthropogenic influences on the SCS. Based on high frequency hydroacoustic profiles (Parasound P70), recorded perpendicular to the coastline with an average spacing of 50 km and a length of 400 km. In addition, a transect of short sediment cores was carried out from the estuary to the deeper sea basin, to investigate the impact of the Pearl river plume on the SCS.

Seismic and hydroacoustic surveys during the cruise could be used to identify suitable coring locations comprising fine-grained deposits at the Pearl river mouth. Short and long sediment cores obtained along the acoustic profiles verified that no further surface layer with muddy sediments was present. Bearing in mind the relative low area coverage by the acoustic investigation and the signal interference due to strong regional gas contents, the current results support the findings of previous studies arguing against substantial deposition of fine sediments on the shelf.

However, preliminary age models and core logging data of two gravity cores from 38 m and 62 m water depth suggest very high detrital sedimentation to be associated with the early Holocene eustatic sea-level rise transgressing the inner shelf area around 11 ka BP (SO269-98-3). High sedimentation rates are maintained throughout the Holocene at the or close to the depocenter of the offshore “mud belt” (SO269-135-3). Compositional changes further reveal a close connection to the orbital paced Holocene SW monsoon dynamics and the inner shelf current regime. Multi-proxy paleoenvironmental reconstructions including biomarkers and inorganic geochemistry on these paired sediment cores are ongoing.

A crustal-like distribution of heavy metals in the surface sediments of the shallower parts of the SCS suggest a limited contribution by Pearl River-derived material at present. In addition to a potentially current-related near-coastal deposition, suspended particulate matter from the Pearl River (H10 cruise) indicates substantial storage of heavy metals such as Cd, Cu, Ni, Pb, and Zn just within the low salinity realm (<10). Contrasting to very low concentrations of dissolved Pb throughout the river, dissolved Zn, Cu, Ni, Cd, and REEs reveal increasing levels in the mid-salinity region ($10-25$). Of the redox-sensitive trace metals, Mo and U show a mostly conservative pattern across the salinity gradient, whereas Re and especially W deviate essentially from this behavior. In the water column of the SCS coastal Ocean, dissolved metals reveal typical patterns including conservative (Mo, Re, U, and W), nutrient-type (Cd, Ni), and surface maxima combined with scavenging and regeneration profiles (Cu, Zn, REE). Interestingly, the surface sediments at greater water depth (>1500 m) are significantly enriched in several metals such as Bi, Cd, Cu, Ni, Sb or Tl compared to the geogenic background. However, a parallel enrichment in redox-sensitive Mo argues against an anthropogenic impact and highlights a natural process related to scavenging by Mn oxides forming at the sediment-water interface as indicated by solid phase Mn and corresponding pore water profiles.

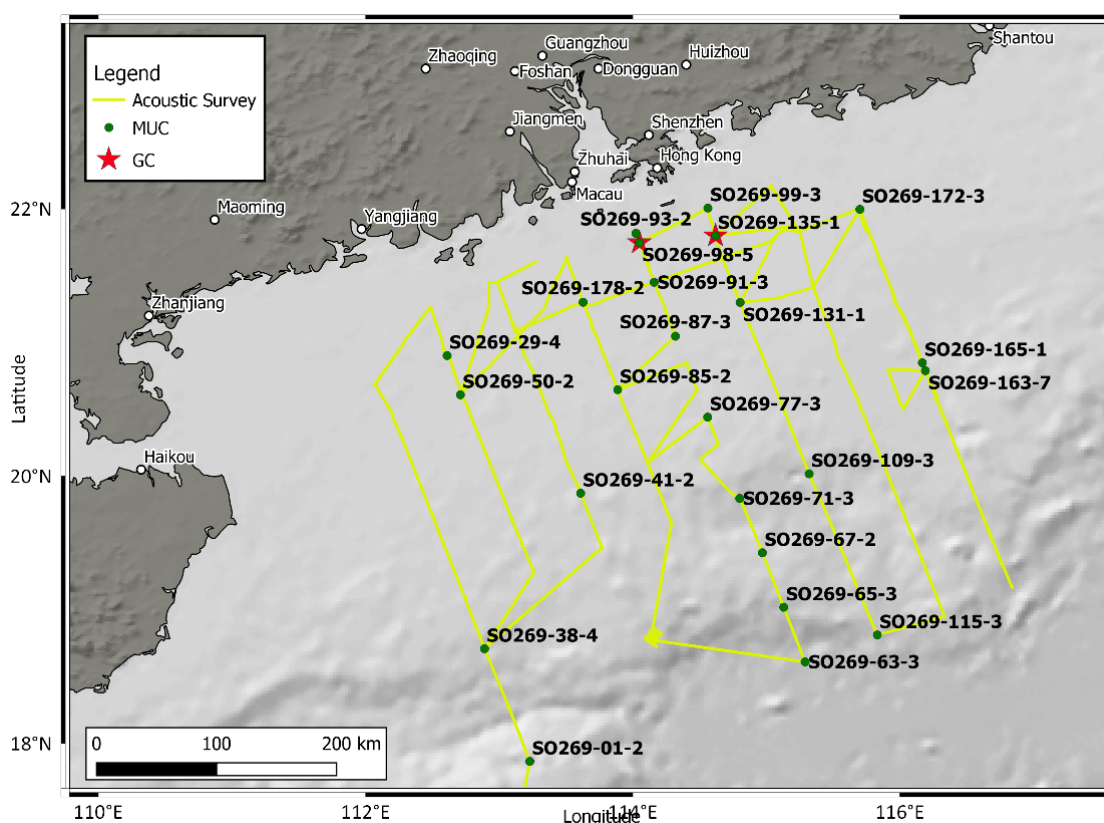


Fig. 10: Map of the research area, highlighting the recorded acoustic transects (yellow lines) and selected working stations (MUC and GC) for detailed analysis. The selected sampling transect is located in the PRE region (Ou et al. 2007), reaching from the river mouth to the deep-sea basin.

2.6 Sedimentary environmental evolution for the past 30 ka on the northern continental slope of the South China Sea (Pingyuan Li¹², Jianfei Lu¹², Zhen Xia¹² and Huayang Gan¹²)

The South China Sea is the largest marginal sea in the Western Pacific. The surrounding land provides massive sediments. Lots of sediments are transported into the deep sea basin through a complex ocean current system through the land slope, and thus the continental slope becomes an important region in the study of deep-sea sediment source and sink system. However, the water depth in the continental slope area varies greatly, the current system in the area is complicated, and the sea level also changes strongly during the glacial-interglacial periods, making the continental slope sedimentary environment study as a hard point.

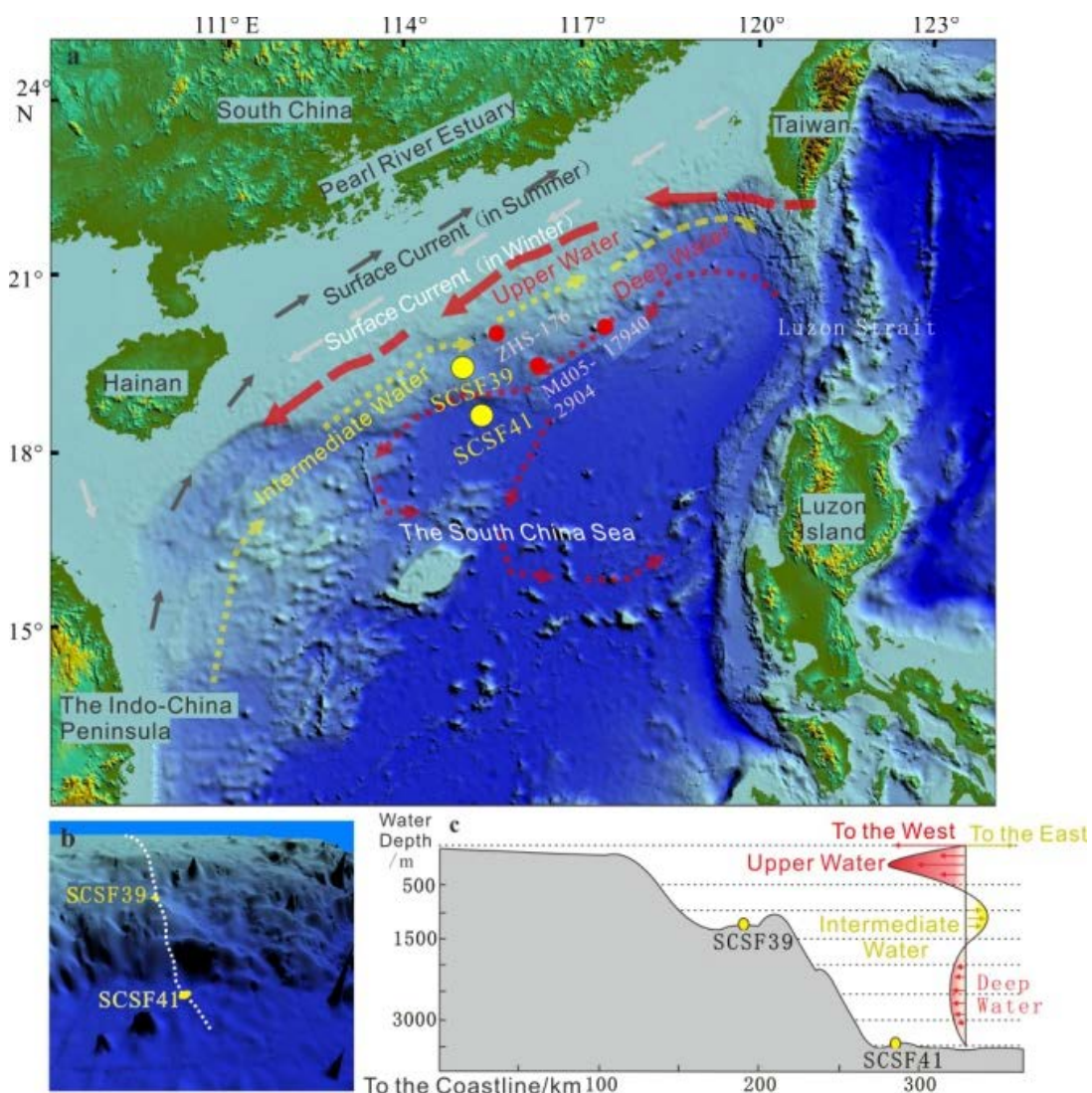


Fig. 11: Topographic map of the studied region.

In order to study the sedimentary environmental evolution on the continental slope, we selected two gravity cores in the continental slope of the Northern South China Sea, one locates at middle of slope, and the other locates at the bottom of the slope (Fig. 11). Through a series of geochemistry analysis, grain size analysis, and dating analysis and previous

studies (ZHAO et al. 2018, WAN & ZHIMIN 2014), the results demonstrate: 1) sea level changes are the dominate factor controlling the changes of terrigenous / biogenous components on the continental slope. The shallow slope region is more sensitive to the sea level changes than the bottom slope region; 2) a carbonate dilution event is found related to the intensification of the East Asia Summer Monsoon during the early Holocene from 11.5 to 8.5 ka B.P (Fig. 12, Fig. 13).

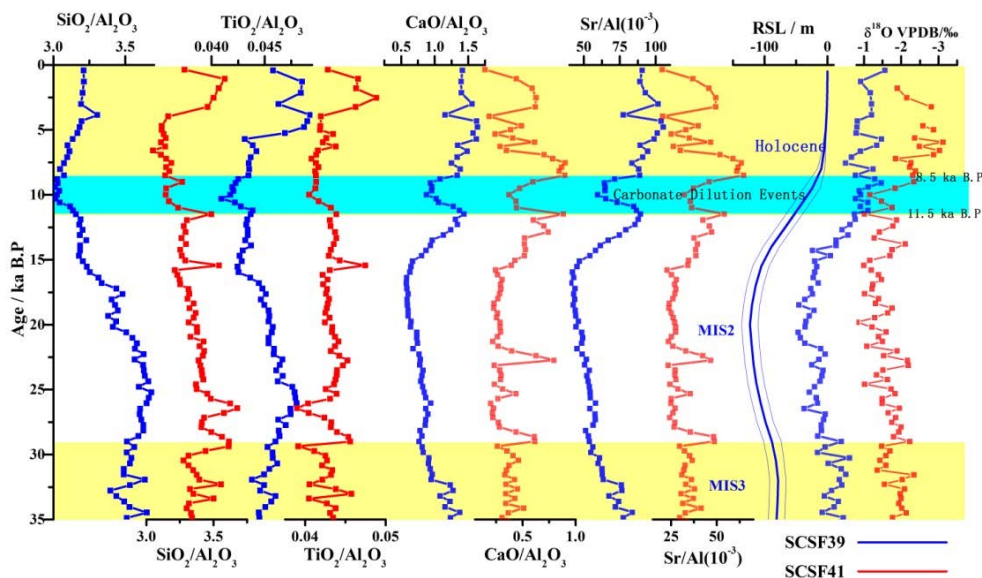


Fig. 12: Geochemical characteristics of the core SCSF39 and SCSF41.

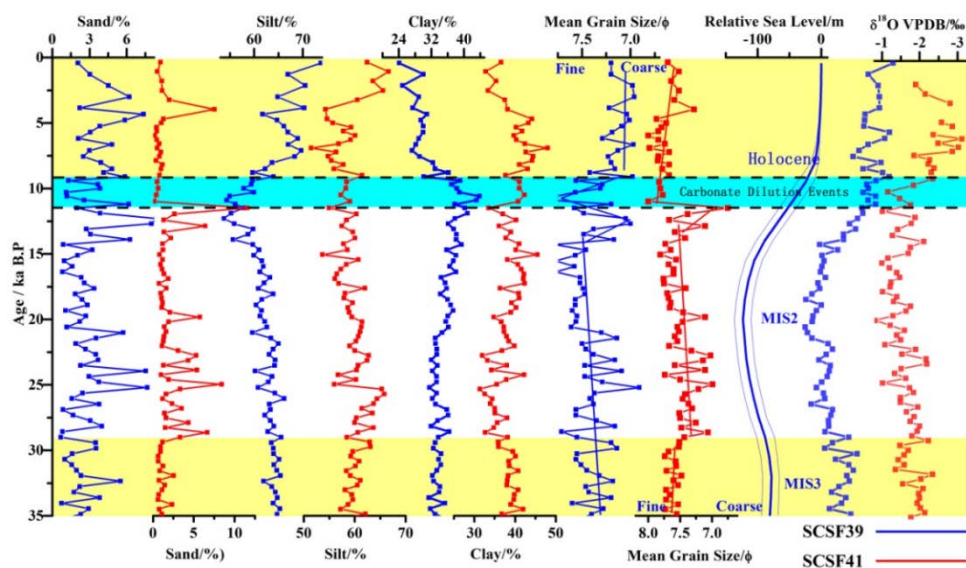


Fig. 13: Grain size distributions of the core SCSF39 and SCSF41.

Acknowledgements:

This study was supported by the Chinese Geological Survey Foundation "A Synthesize Geological Survey Project on the Lingdingyang Area, Pearl River Estuary (DD20190289)."

2.7 Accumulation of recalcitrant organic matter in porewaters in sediment cores of the northern South China Sea (Yunru Chen⁸ and Fengping Wang^{8,7})

During organic matter decomposition in sediments, dissolved organic matter (DOM) is released into the porewater by hydrolysis and depolymerization of particulate organic matter (POM) (SCHMIDT et al. 2017). Therefore, the chemical composition of DOC not only determines the bio-availability of the DOC, but also records the dynamic exchange of organic carbon between POM and DOM. To study the changes of dissolved organic matter under microbial mediation in the sediment cores, Fe(II), sulfate, and dissolved organic carbon (DOC) concentrations in the porewaters were measured, and the optical properties of DOC were characterized by UV-visible absorbance and 3D Excitation-Emission Matrix (3D-EEM). Humification index (HIX) is calculated to represent the extent of humification (WEISHAAR et al. 2003). Specific ultraviolet absorbance at 254 nm is calculated to evaluate the aromatic content (OHNO 2002).

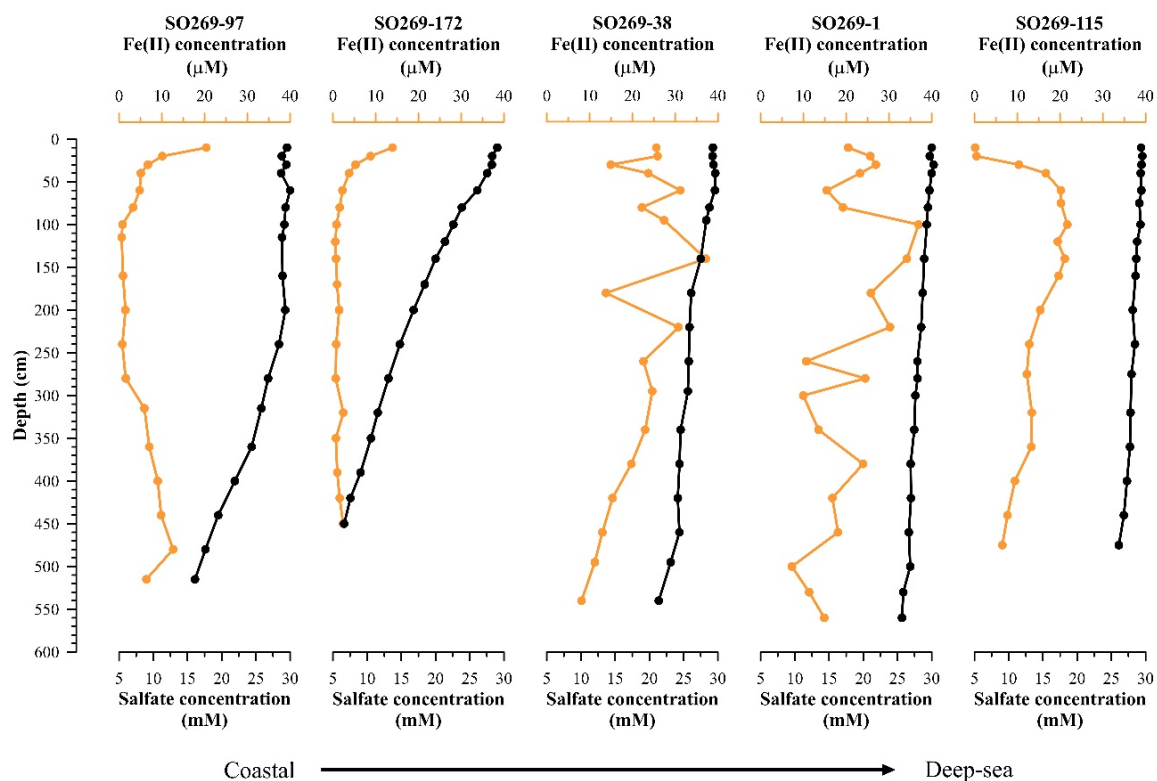


Fig. 14: Fe(II) and sulfate concentration profiles of the sediment cores.

In coastal cores, bio-available Fe(III) was consumed quickly in less than one meter and sulfate consequently serves as the electron acceptor in anaerobic microbial respiration (Fig. 14). In contrast, iron reduction can persist for the upper 5 meters in cores from the continental area and the deep sea, indicating less bio-labile DOC seawards (Fig. 14).

Intriguingly, DOC concentration gradually increased with depth in all sediment cores, showing 2–8 times higher at the bottom than those at the surface. The accumulated DOC was characterized by high humic-like fluorescence (Fig. 15). Meanwhile, downcore increasing

SUVA₂₅₄ shows more significant contribution of the aromatic fraction (Fig. 15). These aromatic compounds may result from microbial degradation of DOC, as the production of aromatic compounds is higher in the coastal area, where stronger microbial activities are expected. The accumulation of these aromatic molecules in core SO269-1 suggests the preferential preservation of recalcitrant compounds in the sediments during long-distance transport.

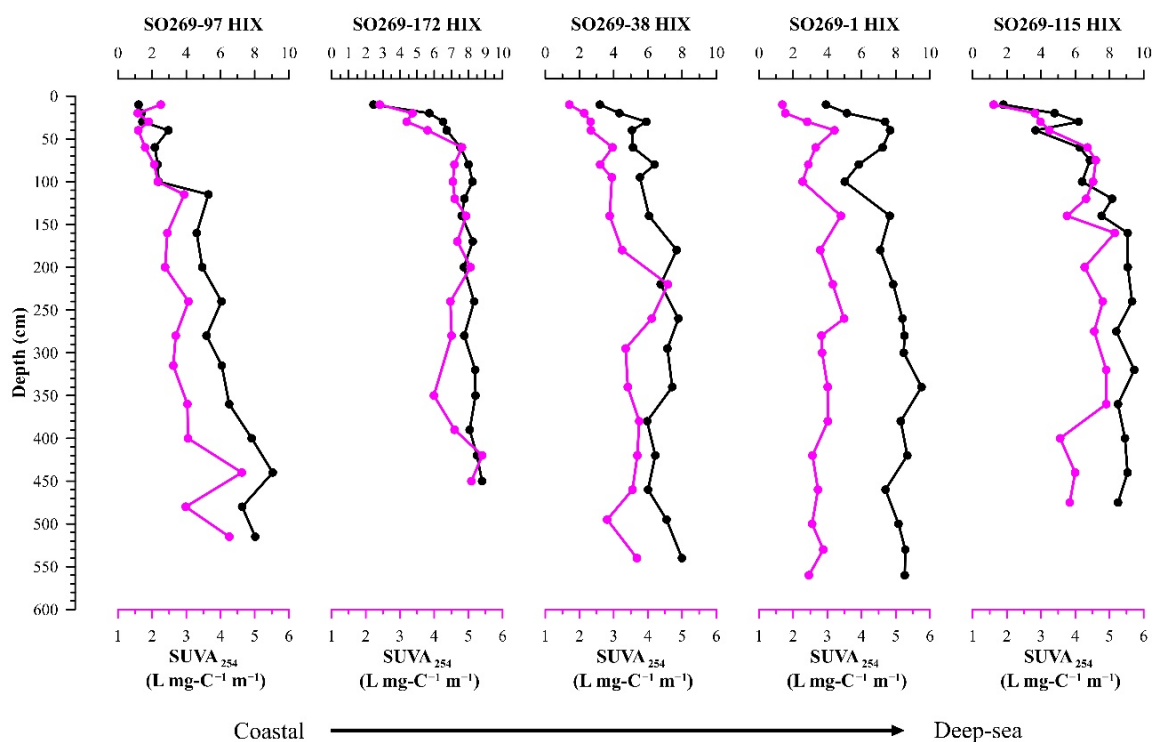


Fig. 15: Humification index (HIX) and specific ultraviolet absorbance at 254 nm [SUVA₂₅₄ ($L\ mgC^{-1}\ m^{-1}$)] profiles of DOC in the sediment core porewaters.

2.8 The nitrogen cycle in the northern South China Sea: Impact of the Pearl River (Jan Maier², Carolin Perkuhn², Shichao Tian², Joanna J. Waniek¹, Niko Lahajnar², Kay Emeis^{2,3} and Birgit Gaye²)

The South China Sea (SCS) is an oligotrophic marginal sea where fixation of atmospheric dinitrogen has been estimated to account for up to 20% of total new production (CHEN et al. 2003, GAYE et al. 2009). The enhanced entrainment of reactive nitrogen from the growing agriculture, land use change, energy consumption, waste and sewage disposal, change nitrogen sources and sinks and locally stimulate eutrophication, especially in the near shore areas off the Pearl River mouth.

In aquatic environments, $\delta^{15}N$ values of dissolved and particulate nitrogen are used to decipher the role of nitrogen cycling processes and to identify nitrogen sources. Most incomplete reactions in the nitrogen cycle are associated with a kinetic fractionation of the stable isotopes ^{14}N and ^{15}N , leading to enrichment of the lighter ^{14}N in the reaction product and

of the heavy isotope in the residual substrate pool (CASCIOTTI 2016, SIGMAN et al. 2005, GAYE et al. 2013). Paired nitrogen and oxygen isotope ratios ($\delta^{18}\text{O}$) of dissolved reactive inorganic nitrogen additionally allow tracking of natural vs. anthropogenic sources of these nutrients and are therefore useful indicators of anthropogenic stress (KENDALL et al. 2007). $\delta^{15}\text{N}$ values below 5‰ of nitrate and sediments particularly in the northeastern SCS were related to high rates of nitrogen fixation in the Western Pacific and import of this signal by inflow of intermediate water masses (CHEN et al. 2003, YANG et al. 2017). $\delta^{15}\text{N}$ values of dissolved reactive nitrogen of 3 to 5‰ within the Pearl River are in a similar range as the values of the marine end member. However, isotope fractionation by nitrogen assimilation leads to enhanced $\delta^{15}\text{N}$ values up to 9‰ off the river mouth (YE et al. 2015).

The aim of this study is to improve the existing concepts of nitrogen transport and nitrogen cycling in the northern SCS and to estimate the impact of the anthropogenic enhancement of aeolian and riverine nitrogen supply. Water and suspended matter (SPM) were sampled during the research cruise SO 269 along a grid off the Pearl River mouth extending to the lower continental slope. $\delta^{15}\text{N}$ values of dissolved reactive and particulate nitrogen have been investigated and results of stable nitrogen isotope analyses are presented.

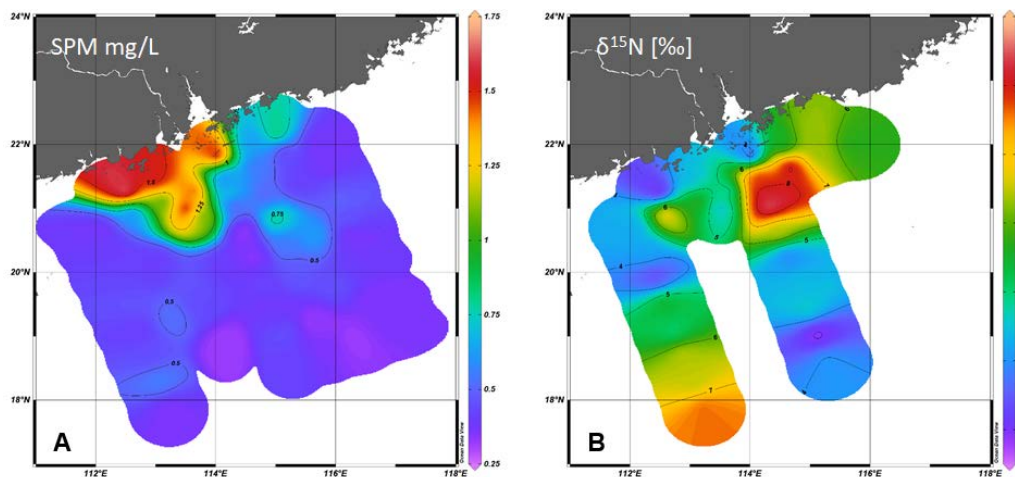


Fig. 16: Suspended matter concentrations (SPM) in surface waters in the northern SCS off the Pearl River mouth (A) and $\delta^{15}\text{N}$ [‰] values of suspended particulate nitrogen close to the coast and along two offshore extending transects (B).

The river plume is delineated by reduced salinities as well as enhanced nutrient and SPM concentrations in the upper 10 m of the water column (Fig. 16A, B). The riverine nutrients cause enhanced productivity with $\delta^{15}\text{N}$ values below 5‰ in the surface SPM due to the prevailing fractionation effect ($^{15}\epsilon$) of 3‰. The strong increase of $\delta^{15}\text{N}$ values at the margins of the river plume are due to the uptake of residual nitrate, which has become isotopically enriched up to $\delta^{15}\text{N}$ values > 8 ‰. Outside the area impacted by Pearl River discharge, subsurface waters are the major nutrient source. This is indicated by deep chlorophyll maxima dropping from 40 m depth near shore to 80 m offshore. The $\delta^{15}\text{N}$ values of SPM 4–7‰ within this chlorophyll maximum reflect those of subsurface nitrate (YANG et al. 2017). Although the

riverine and marine end-members have quite similar $\delta^{15}\text{N}$ values in the study area, the position of the chlorophyll maximum allows distinguishing these nutrient sources.

Acknowledgements:

We thank the BMBF for funding the sampling campaign in the South China Sea within the joint Sino-German project MEGAPOL with the subproject SOCLIS-N carried out at the University of Hamburg (BMBF grant 03G0269B). We further thank the BMBF for funding the PhD position of Shichao Tian within a complementary study in the Bohai and Yellow seas by the project FINGNUTS (BMBF grant 03F0786B). We are indebted to officers and crew of RV SONNE for their help during sampling on board. We are grateful to Markus Ankele, Jenny Jeschek, Lars Kreuzer, Sigfried Krüger, Frauke Langeberg, Robert Mars, Birgit Sadkowiak, and Ingo Schuffenhauer for technical support and laboratory analyses.

2.9 Estrogenic compounds in the Pearl River Estuary and coastal South China Sea (Carina Deich¹, Marion Kanwischer¹, Helena C. Frazão¹, Jana-Sophie Appelt¹, Ruifeng Zhang⁷, Wenguo Li⁴, Thomas Pohlmann⁴ and Joanna J. Waniek¹)

Densely populated regions such as the area around the Pearl River Estuary are suspected of exerting considerable anthropogenic pressure on the surrounding environment. It has been found that modern pollutants can be transported into rivers and thus into the marine environment via sewage treatment plant effluents as well as through incorrect disposal of industrial waste (YING et al. 2002, YING et al. 2008). Estrogenic substances have gained concern as they interact with the hormone system of organisms, where they can cause adverse health effects. They are therefore categorized as endocrine disrupting compounds (EDCs). For example, MORTHORST et al. (2014) showed that the natural estrogen estradiol adversely affects embryos of the viviparous eelpout (MORTHORST et al. 2014).

In this study, we analyzed surface water samples taken along the salinity gradient of the Pearl River Estuary (PRE) and from the northern South China Sea (SCS; Fig. 17A) for six target analytes, i.e., estradiol, estrone, ethinylestradiol, daidzein, genistein and zearalenone. The samples were investigated via instrumental analysis on a liquid chromatography–tandem mass spectrometry system.

Natural estrone was detectable at all stations in the PRE and at most stations in the SCS (Fig. 17B, Fig. 18). Natural 17β -estradiol was not detected in the PRE, but occurred in the SCS at stations close to the coast in August 2019. Synthetic ethinylestradiol was only present in the PRE at the sampling site closest to the South China Sea (Fig. 17B). Comparatively high 17α -ethinylestradiol concentrations were measured in the SCS during both sampling campaigns at stations close to the coast. Daidzein, genistein and zearalenone were detected at most stations in the PRE, but only genistein occurred at one station in the SCS. In general, estrogen concentrations in the estuary declined towards the sea except for the station close to the estuary's mouth (PR-1; Fig. 17B). In the SCS, the surface density and the modeled surface

currents indicate an influence of the Pearl River plume on the stations close to the coast. This could explain the observed distribution patterns of estrogens. Also, the distribution patterns show regional and inter-annual variability presumably arising from the prevailing monsoon.

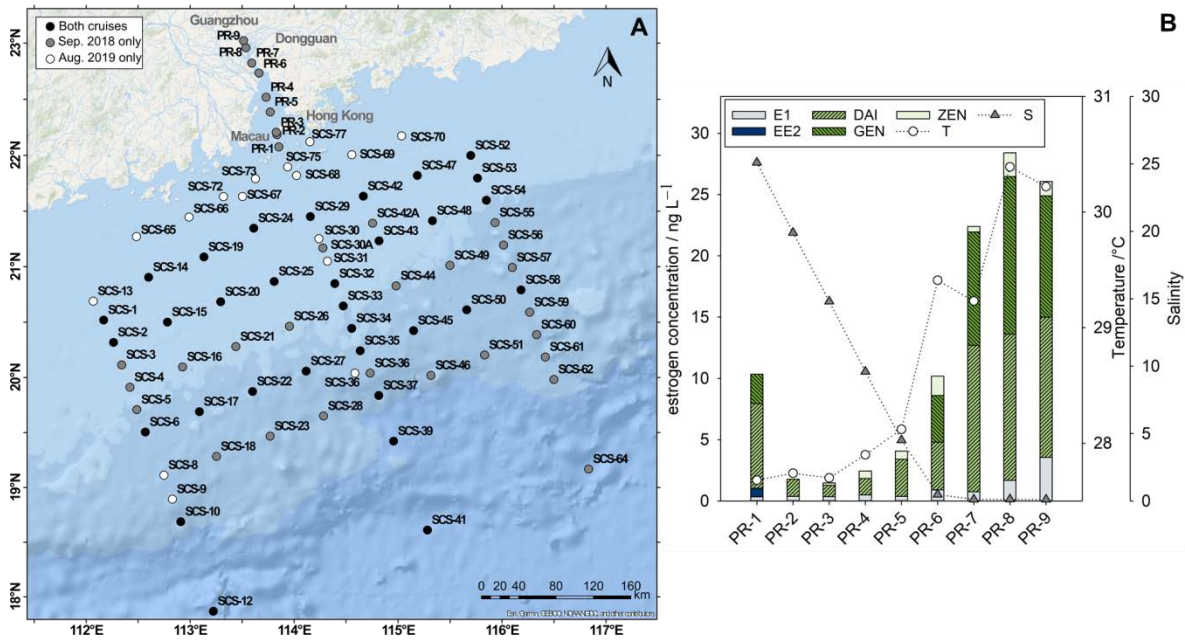


Fig. 17: Study sites in the northern South China Sea (A). Concentrations of estrone (E1), 17 β -estradiol (E2) and 17 α -ethinylestradiol (EE2), daidzein (DAI), genistein (GEN) and zearalenone (ZEN) in the Pearl River Estuary (2018) with surface water temperature and salinity (B).

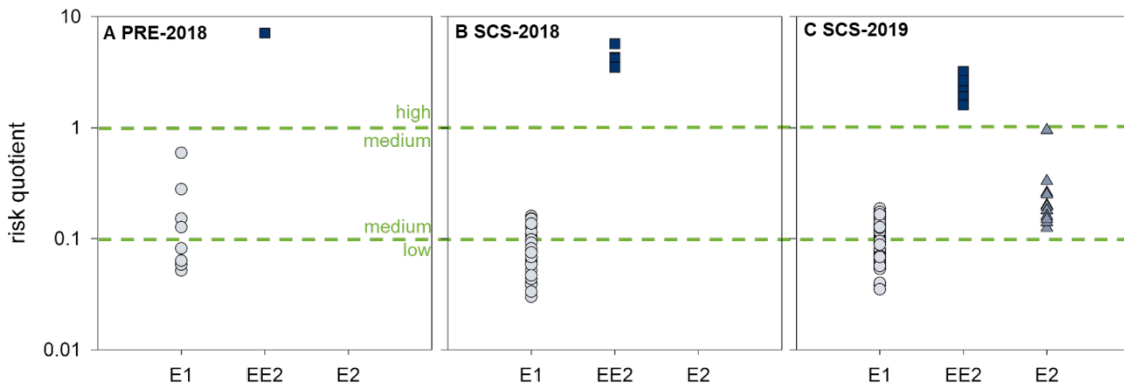


Fig. 18: Risk quotients based on E1, E2 and EE2 in surface water samples from A) the Pearl River Estuary (2018) and from the northern South China Sea in B) 2018 and C) 2019.

Risk quotients based on compound specific predicted no-effect concentrations were calculated to estimate the potential risk to which marine organisms could be exposed. The natural steroids estrone and 17 β -estradiol concentrations indicate a low to moderate risk to aquatic organisms, while synthetic 17 α -ethinylestradiol concentrations indicate a high ecotoxicological risk in freshwater and saltwater (Fig. 18).

Acknowledgements:

We would like to thank the participants and the crew of the cruises on Hai Yang Di Zhi Shi Hao in September 2018 and on board of SONNE-269 in August 2019. This research is part of the Sino-German project MEGAPOL which received funding from the BMBF under contract numbers 03Fo786A and 03Fo786B as well as 03Go269 (SONNE-SOCLIS).

2.10 Distribution patterns of organic pollutants in water and sediment samples of the South China Sea (Kathrin Fisch¹, Ines Hand¹, Maike Wilschnack¹ and Detlef E. Schulz-Bull¹)

In the Pearl River Estuary (PRE), a megacity is currently emerging, which puts high anthropogenic pressure on the ecosystem of the estuary and the northern South China Sea (SCS).

The aim of this study was to analyze the anthropogenic fingerprint of the Pearl River plume on the northern South China Sea. To reach this goal, we analyzed 15 polycyclic aromatic hydrocarbons (PAH), 4 dichlorodiphenyltrichloroethane's (DDT), 24 polychlorinated biphenyls (PCB), and 40 pharmaceuticals and personal care products (PPCP) in the water and sediment of the northern SCS. All samples were taken during the cruise with R/V Hai Yang Di Zhi Shi Hao in September 2018.

PAHs, PCBs, and DDTs belong to the group of persistent organic pollutants (POPs) and have been monitored in the environment for several decades. Whereas, PPCPs belong to the group of contaminants of emerging concern and have only been studied in the environment in the last decade.

Of the 40 analyzed PPCPs, only three pharmaceuticals and two UV-Filters were detected in the surface water of the northern SCS, and 14 in the Pearl River Estuary at low ng/L concentrations (parts will be published in (FISCH et al. 2021)). In the Pearl River, clear distribution patterns could be detected for the pharmaceuticals, yet not for the UV-Filters. The pharmaceuticals either originate from the domestic wastewater or intensive livestock industry. Whereas UV-Filters possibly originate from diffuse sources. The PPCPs in the northern SCS do not display a distinguishable distribution pattern. However, their detection can lead to the conclusion that they could be more stable in the marine environment than expected (FISCH et al. 2021).

Sediment samples were analyzed for PAHs, PCBs, DDTs, and PPCPs (Fig. 19A–D). The general distribution pattern shows that higher concentrations tend to occur in the eastern part of the working area. This is the first time that PPCPs were analyzed, in sediments of the SCS. The PPCP distribution pattern displays elevated concentrations at the edge of the shelf and lower concentrations on the shelf. The distribution pattern of the PAHs and DDTs is similar to the previously reported distribution pattern of KAISER et al. (2018) from a cruise in spring 2015 (KAISER et al. 2018).

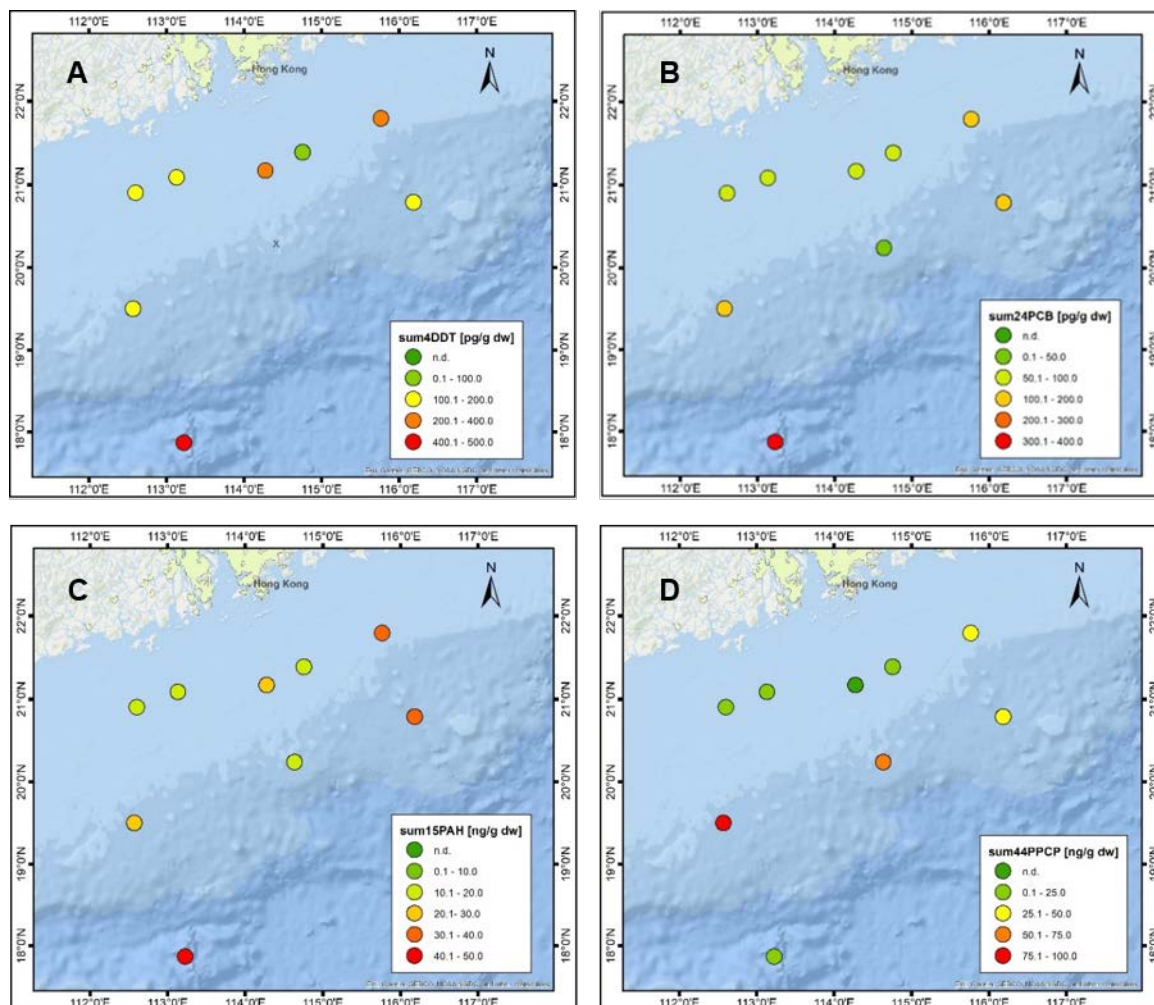


Fig. 19: Sum of organic pollutants concentrations in the sediment of the northern South China Sea of A) DDTs (x - sample was contaminated), B) PCBs, C) PAHs, D) PPCPs; (preliminary data).

Acknowledgements:

The authors thank all scientific and ship crew members of the R/V Hai Yang Di Zhi Shi Hao. Furthermore we would like to thank Astrid Lerz and Andrea Tschakste for the sediment extractions of the POPs.

2.11 Environment evolution and ecological impact of oxygen-depleted waters in the Pearl River Estuary and coastal area, China (Dehao Tang^{12,13}, Yugen Ni^{12,13}, Gaowen He^{12,13} and Zhen Xia^{12,13})

The rapid industrialization and socioeconomic development during the past 40 years had a substantial impact on the environmental change of Pearl River estuary, which included eutrophication, hypoxia area, increased persistent organic pollutants (POPs), and sedimentary environmental evolution (DIAZ & ROSENBERG 2008, LAFFOLEY & BAXTER 2019). The Pearl River discharged a large load of nutrients and anthropogenic contaminants into the estuary, which could have resulted in hypoxia and organic pollutants (Fig. 20).

We aim to solve three key scientific problems: (1) revealing the spatial and temporal distribution characteristics of hypoxia area in the Pearl River Estuary and its adjacent sea areas; (2) identifying the historical trend of hypoxia in the study area: applications of chemical biomarkers and microfossils; (3) revealing environmental evolution and impacts of human activities in recent hundred years, especially the ecological impact of hypoxia area in the Pearl River Estuary.

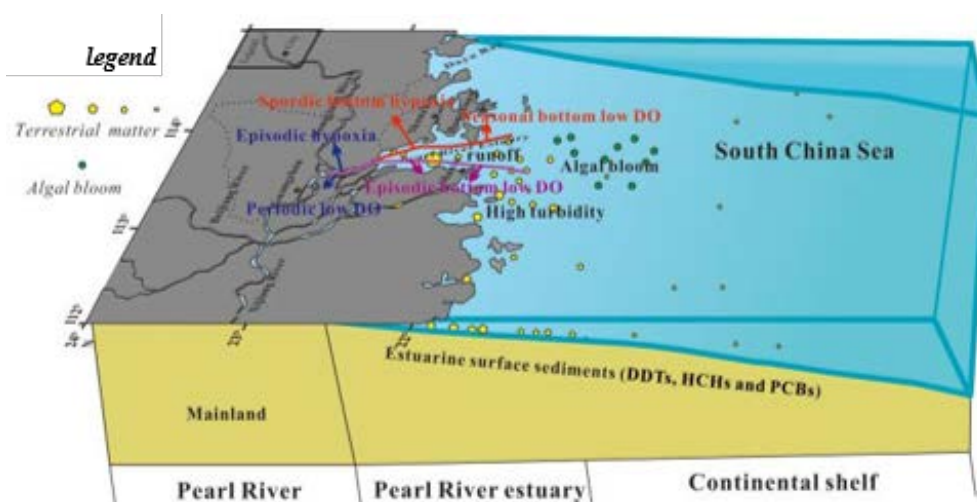


Fig. 20: Hypoxia in the Pearl River estuary and its adjacent sea areas.

In this proposal, (1) Continuous time series data was used to examine the spatial and temporal distribution of dissolved oxygen (DO) and other water quality parameters in the Pearl River Estuary and its adjacent sea areas. The main estuary section had been experiencing episodic events of low DO and sporadic hypoxia during the years of 1988–2011. Downstream of the main estuary section in the eastern shelf, the bottom waters experienced low DO, but hypoxia seldom occurred, whereas low DO rarely occurred in the western shelf (LI et al. 2020). (2) We will utilize plant pigments, lignin-phenols, stable isotopes ($\delta^{13}\text{C}$ and $\delta^{15}\text{N}$), and foraminiferal microfossils in ^{210}Pb dated cores to examine the history of hypoxia in the study area. The abundance of plant pigments, which are indicators of enhanced diatom and cyanobacterial abundance, agrees with the record of increasing nutrient loads in study area in ^{210}Pb dated cores. Lignin data can reflect enhanced loading of woody materials. Carbon and nitrogen parameters (stable isotopes, OC, C/N ratios) can reflect relative differences in the amount of carbon tracked by these different proxies. And increases in low-oxygen tolerant foraminiferal microfossils indicate there has been an increase in the number of hypoxic bottom water events (LI et al. 2011, JIA & PENG 2003). (3) We will compare the differences of external environment indicators and internal ecosystem structure, function and energy transformation between the hypoxic stations and non-hypoxic stations (TANG et al. 2018), and analyze the impact of hypoxia on ecosystem and marine economy. Environmental indicators at the hypoxic stations, including water quality, surface sedimentary environment, and pollutant content, are significantly different from those in non hypoxic areas. The distribution, sources, and ecological risks of organochlorine compounds (DDTs, HCHs, and PCBs) in surface sediments from the Pearl River Estuary were positively correlated with the location of

low DO area in 2017 (Fig. 21a–c; LI et al. 2020, TANG et al. 2020). However, more demonstration and long-term data support are still needed. At the hypoxic stations, the biomass of mesozooplankton was relatively higher and the taxonomic diversity of mesozooplankton was lower (SHI et al. 2019). Meanwhile, the structure, function and eco-exergy level of benthos and nekton communities will change accordingly. Hypoxia will affect the development of marine ecosystem and marine economy, especially the mari-culture industry.

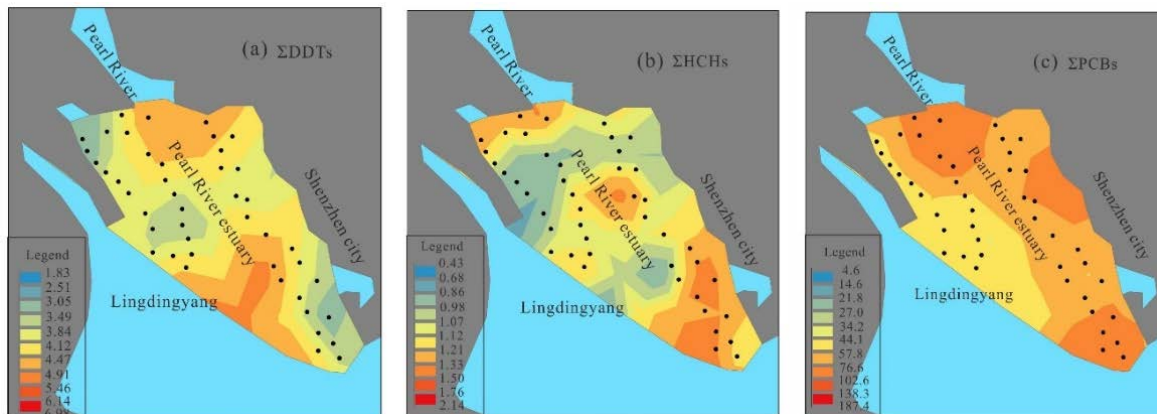


Fig. 21: (a) Distribution of the DDTs concentration, (b) HCHs concentration and (c) PCBs concentration; all units are $\text{ng}\cdot\text{g}^{-1}$ d.w.

Acknowledgements:

This work was supported by the Natural Science Foundation of China (NSFC) (No. 41806130), the Southern Marine Science and Engineering Guangdong Laboratory (Guangzhou) and Project of China Geological Survey.

2.12 Benthic foraminifera as bioindicators off the Pearl River Estuary (South China Sea): baseline study and potential application (Jassin Petersen¹¹, Julian Pietralla¹¹, Tamara Hechemer¹¹, Johanna Schmidt¹¹, Anna Saupe¹¹ and Patrick Grunert¹¹)

Reconstructions of oceanographic parameters (e.g., nutrient supply and oxygen availability) along continental margins are contributing to the refinement of projections of future climate states in a warming world. Global warming combined with the growth of densely populated coastal areas, e.g., in the Guangzhou-Hong Kong megacity, is thought to adversely affect related marine ecosystems. Regarding reconstructions, benthic foraminifera have been established as good indicators of marine environmental status on a range of spatial and temporal scales due to (amongst others) the excellent preservation potential of their shells in the fossil record.

In this study, we investigate the recent fauna of benthic foraminifera from the northern shelf of the South China Sea (SCS) in close proximity to the Pearl River Estuary (PRE). By defining ecological groups based on the recent fauna along a bathymetric transect ranging from the shelf to the deep sea we provide a baseline for the use of these bioindicators for (high-

resolution) reconstructions of environmental change in the past in this sensitive marine realm (Fig. 22). A similar approach has proven successful, e.g., in the south-western SCS for identifying relatively short-term changes in ocean circulation dynamics as induced by the seasonally changing monsoon patterns (SZAREK et al. 2006, SZAREK et al. 2009). We aim at refining local transfer functions based on the faunal composition for estimating important paleoceanographic parameters such as paleoproductivity.

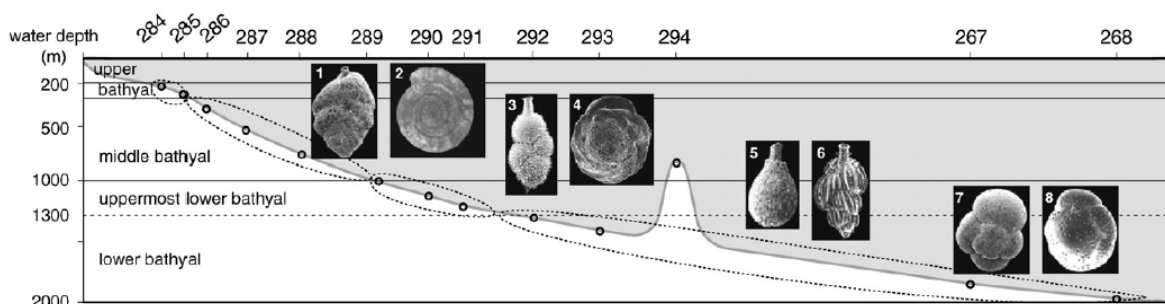


Fig. 22: The succession of the benthic foraminiferal faunal composition along a transect on the Sunda shelf (southern SCS) is displayed here exemplarily by the dominant species for contrasting depth ranges. Taken from SZAREK et al. (2009), where a detailed description is given.

We will apply existing and newly developed transfer functions to new core material from the study area to investigate changes in productivity and oxygenation at the seafloor on Holocene timescales. The results can be compared to existing proxy studies of the northern SCS in order to highlight spatial variability of these parameters (e.g., WANG et al. 2018), and can also be transferred to similar ecosystems in other regions. It shall assist in constraining the environmental variability, for an area presently affected by sedimentation from the PRE, throughout the Holocene on a regional to local scale compared to the present state as well as to what can be expected and modeled in future climate change scenarios.

2.13 Vertical Distribution and Size Structure of Zooplankton in Different Water Column in the Northern South China Sea (Kaixuan Chen⁷, Meng Zhou⁷, Joanna J. Waniek¹, Yisen Zhong⁷ and Yiwu Zhu⁷)

The South China Sea is the third largest marginal sea in the world. There are many studies that work on spatial variation of zooplankton using traditional plankton sampling methods in northern South China Sea, which leads to less researches about high-resolution vertical distribution of zooplankton (LI et al. 2006, ZHANG et al. 2009, ZHOU et al. 2015, ZHANG et al. 2019). We utilize the Laser Optical Plankton Counter (LOPC) that measures zooplankton size range between 100 μm and 35 mm to explore the vertical distributions and size structures of zooplankton in the Northern South China Sea during summer 2018 (HERMAN 1983, HERMAN et al. 2004). We found that the vertical distribution of zooplankton in different water columns is significantly different (Table 2, Fig. 23). The abundance and the biomass concentrations of zooplankton significantly correlated with buoyancy frequency (N_z) in stratified water.

Moreover, small zooplankton between 100 and 500 μm had a higher correlation with stratification than large zooplankton. For smaller zooplankton, they are more likely to be affected by stratification because of their weak swimming ability. While for large zooplankton, they have strong mobility and easier to traverse different density layers, they can have a broad distribution in the water column. At the same time, the water column was fully mixed and stratification disappeared at the stations after the typhoon. In the mixed water column, zooplankton were not concentrated in the pycnocline and evenly distributed from surface layer to the bottom.

Table 2: Correlation coefficient between zooplankton biomass and buoyancy frequency.

Size range	Stratified water	Mixed water
100-200 μm	0.4497**	0.0915
200-500 μm	0.3091**	-0.0377
500-1000 μm	0.1598**	-0.1037*
1000-2000 μm	0.0799	-0.0458
2000-20000 μm	-0.1310	-0.0319

(Pearson correlation analysis, ** $p < 0.01$, * $p < 0.05$)

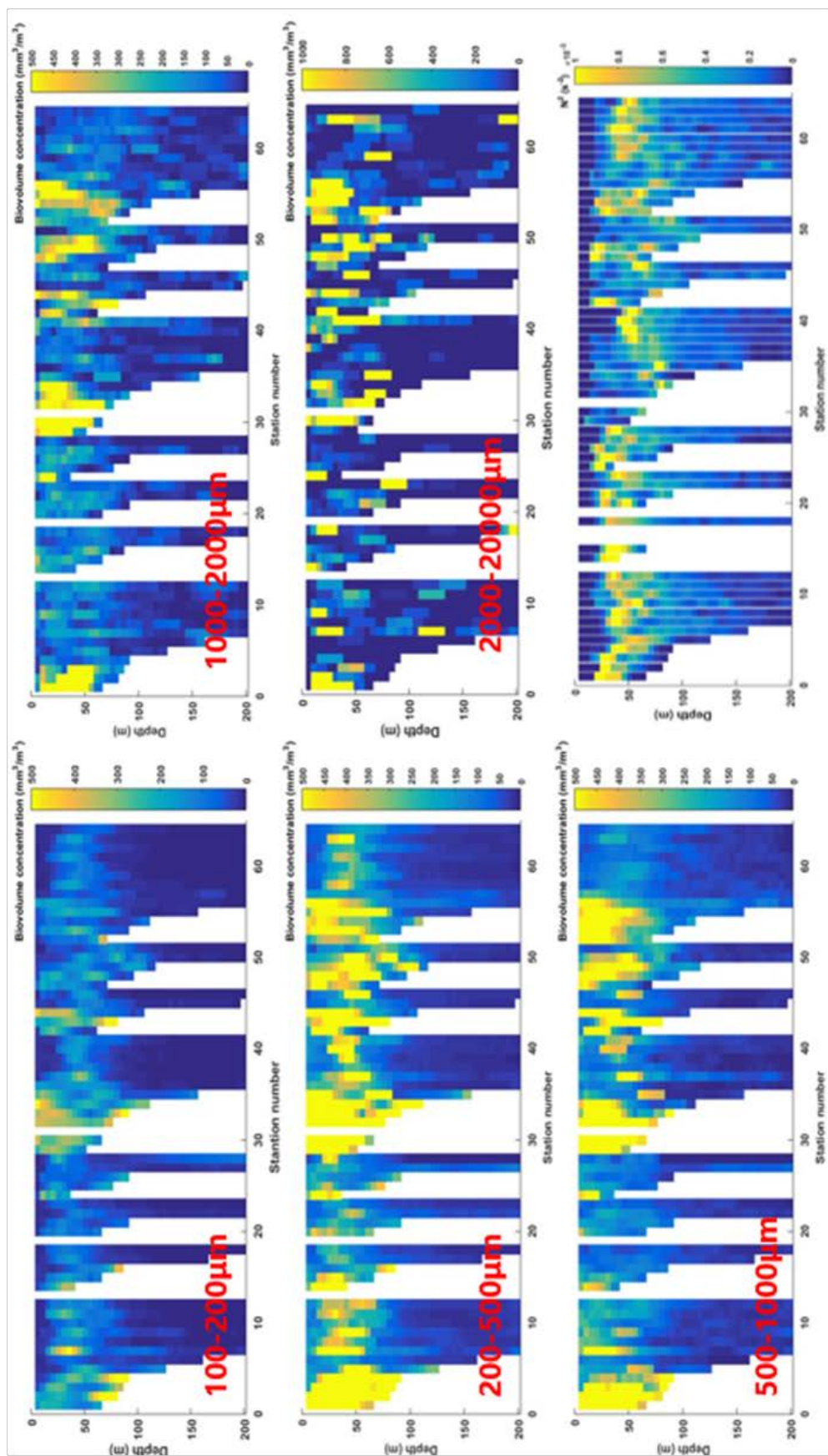


Fig. 23: Biovolume vertical distribution of different size groups and the N_2 distribution.

3 Investigations of pollutants dispersal in the Bohai and Yellow Sea

The Bohai Sea and the Yellow Sea, as well as the adjacent East China Sea to the south, are shallow marginal seas of the Northwest Pacific Ocean and are in focus in this chapter. They lie almost entirely on the Northeast Asian Shelf. While the Yellow Sea and East China Sea are characterized by strong exchanges with the Pacific Ocean due to their open seaward margins, the Bohai Sea is a relatively closed sea with limited exchanges with the open ocean via the 100 km wide Bohai Strait. Ocean currents throughout the region are dominated by alternating summer and winter monsoons. Combined with the shallow depth of these marginal seas of less than 50 m in many parts and the large changes in water and nutrient inputs, significant ecosystem changes are occurring. In recent decades, riverine inputs have greatly decreased, resulting in increased salinity and decreased inputs of phosphate and silicate. At the same time, inputs of reactive nitrogen from wastewater and fertilizers have increased tenfold (Ning et al. 2010; Zhang et al. 2004; Zhao et al. 2002). Severe eutrophication especially in the river plumes of the Yellow River and the Yangtze River is the result, which seasonally leads to the development of so-called oxygen-free death zones (Chen et al. 2014). Nutrient inputs will further increase with the planned Bohai Rim Urban Agglomeration/ Northern Yellow Sea, further driving eutrophication and oxygen depletion.

3.1 Numerical simulation of pollution's transportation on the East Chinese Shelf and in the northern South China Sea (Wenguo Li⁴, Bernhard Mayer⁴ and Thomas Pohlmann⁴)

A large amount of anthropogenic pollution enters into ocean through rivers, threatening the health of marine ecosystem. In order to trace chemical and biogeochemical pollution caused by rapid development of coastal cities in China, numerical simulations were carried out for the East China Sea (117°E–131.2°E, 23°N–41.1°N) and northern South China Sea (105°E–121°E, 13°N–24°N), respectively, using the regional 3D hydrodynamic prognostic Hamburg Shelf Ocean Model (HAMSOM) and a Lagrangian tracer model. The HAMSOM model was applied to produce the hydrodynamic forcing for the tracer model. Pollution was simulated by means of passive tracers.

These were released next to the Yangtze River, Yellow River and Pearl River mouths. Two releasing scenarios for tracers were set up: (1) daily release of a single tracer to investigate their trajectories; (2) release of a number of tracers at a certain time to calculate their residence time.

As shown in Fig. 24A–C, trajectories of tracers released in different months were compared, especially for winter and summer seasons. Tracers released near the Yangtze River and Pearl River mouths follow different trajectories in winter and summer, while tracers released near Yellow River mouth share similar trajectories for both seasons.

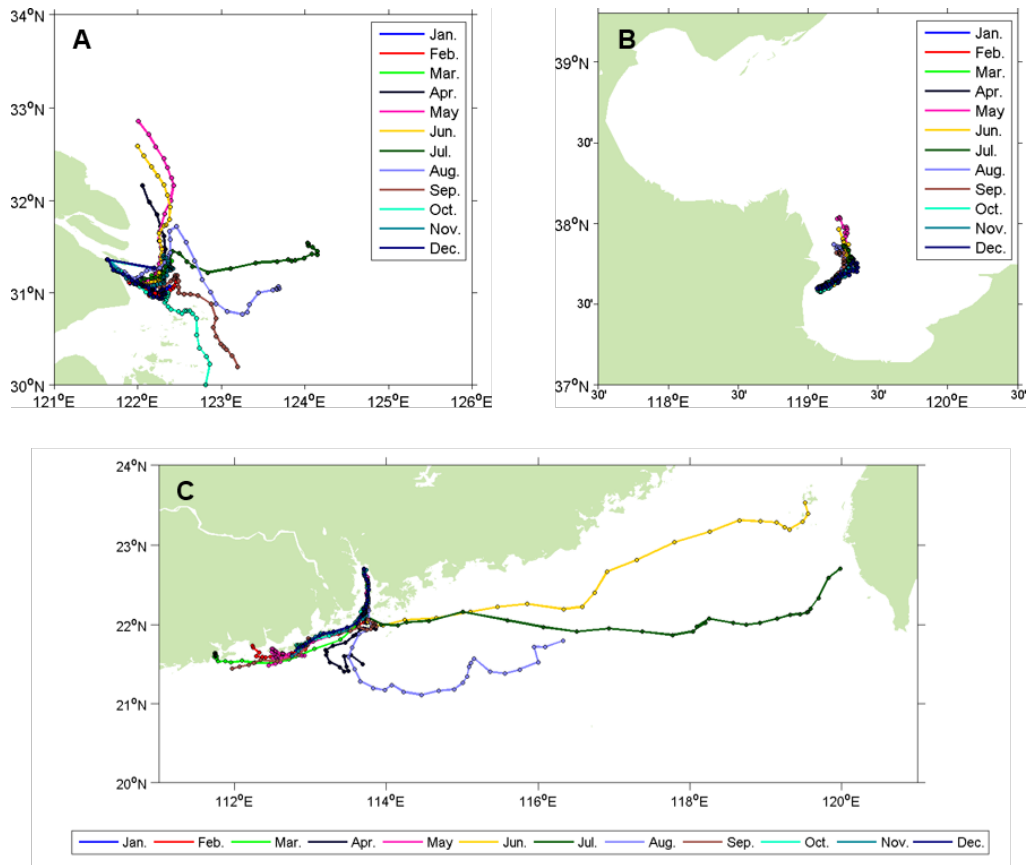


Fig. 24: Trajectories of tracers released at the first of each month at A) Yangtze River, B) Yellow River and C) Pearl River mouths with a travel time of 30 days.

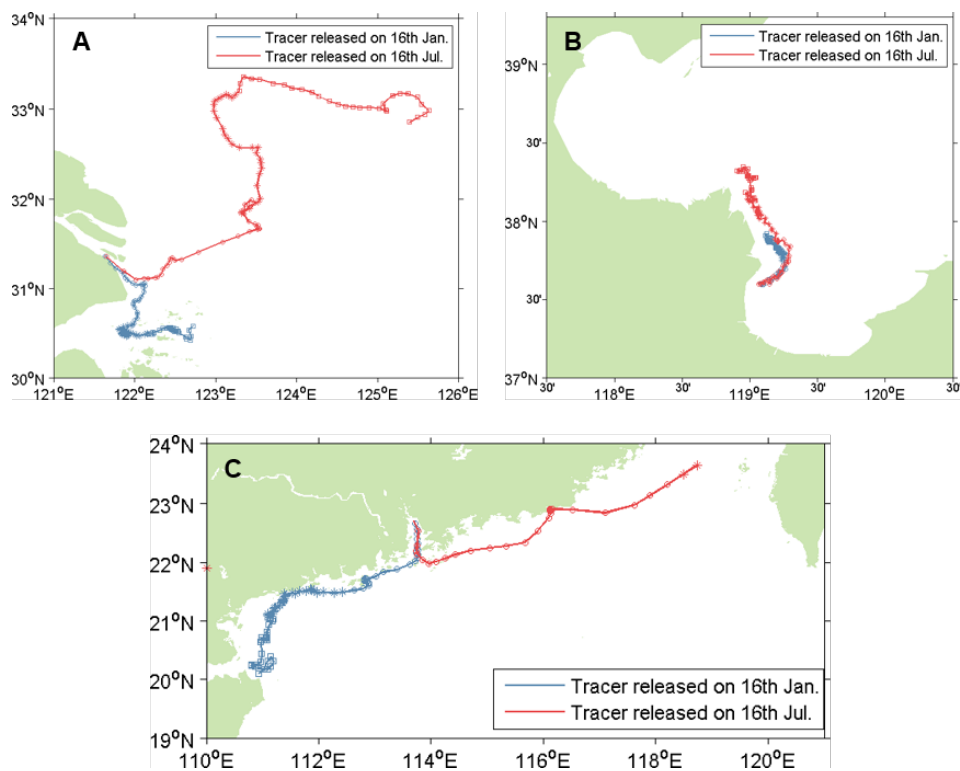


Fig. 25: Trajectories of tracers released on 16th January and 16th July at A) Yangtze River, B) Yellow River and C) Pearl River mouths with a travel time of 90 days. Tracers are marked with different markers (in the order of circle, asterisk, and square) every 30 days.

As shown in Fig. 25A–C, the tracer released near the Yangtze River mouth on 16th January moves southeastward, while the one released on 16th July first moves southeastward and then turns northward and finally turns to eastern direction. The tracer released near the Pear River mouth on 16th January moves westward along the coastline and then turns southward till the northern tip of Hainan Island, while the one released on 16th July moves northeastward towards the Taiwan Strait. However, the tracers released near the Yellow River mouth on 16th January and 16th July share similar trajectories, i.e. first move northeastward and then turn northwestward. In addition, the tracers are marked with different markers every 30 days to more clearly indicate their movement with time. It can be deduced that tracers released in summer move much faster than those released in winter for all of these three river mouths.

The movement of tracers is mainly determined by the local current field which can be deduced from the comparison of tracer trajectories and the monthly current fields. In turn the current fields around these river mouths are mainly influenced by tides, the surface wind and the local density gradient. The residence time of tracers in a local $1^{\circ}\times 1^{\circ}$ box area amounts to 29 days in winter and 12 days in summer at the Yangtze River mouth; 115 days in winter and 56 days in summer at the Yellow River mouth; 22 days in winter and 9 days in summer at the Pearl River mouth.

3.2 The budget of nitrate isotopes in Bohai Sea based on an isotopic balance model (Shichao Tian², Birgit Gaye², Jianhui Tang⁹, Yongming Luo¹⁰, Tina Sanders³, Kirstin Dähnke³ and Kay-Christian Emeis^{2,3})

During the last 40 years of the 20th century, strong anthropogenic activity induced severe environmental changes in the Bohai Sea (BHS) increasing salinity, temperature, DIN and N/P ratios (NING et al. 2010, ZHANG et al. 2004, ZHAO et al. 2002). DIN increased by 3–9 times during 1982–2009, while phosphate and silicate decreased by 2–6 times so that DIN/P increased by about 30 times (LIU et al. 2011, ZHANG et al. 2004). In 2018, we carried out two sampling campaigns in order to identify recent trends of nutrient supply and associated anthropogenic stress within the BHS.

According to our survey, the average value of nitrate in 2018 is $4.20\ \mu\text{mol/L}$, which is higher than the average nitrate concentration of $3.55\ \mu\text{mol/L}$ measured in the 1990's (ZHANG et al. 2004). Nitrate budgets reported during last two decades were not completely constrained because lack of data (LIU et al. 2009, LIU et al. 2011, LIU et al. 2003, ZHANG et al. 2004). To alleviate this lack, we further use stable nitrogen isotopic ratios ($\delta^{15}\text{N}$) of dissolved reactive and particulate nitrogen to quantify the sources and sinks of nitrogen in the present BHS.

A first box model of the BHS nitrate budget following the LOICZ approach balanced sources and sinks of nitrate (ZHANG et al. 2004). In this study, we develop a combined mass and isotope box model entailing new data on the $\delta^{15}\text{N}$ values of nitrate, suspended matter and surface sediments and new data on river discharge and submarine ground water (SGD) nitrogen supply. The approach using nitrate isotopes is helpful to close the nitrate budget,

which can hardly be constrained by only a nitrate mass balance. We propose an updated N-budget that is internally consistent. According to our calculation, the river and SGD discharge comprise 62.8% of the total input of nitrate while the atmospheric supply contributes 25.0%. Benthic diffusion of nitrate, nitrified from ammonium released during the remineralization of organic matter supplies 12.1% to total nitrate of the BHS. Meanwhile, sedimentation removes 91% of the nitrate in BHS, whereas water exchange with the Yellow Sea leads to a net loss of 5.4% of the total nitrate. The benthic flux of nitrate from water to sediments is the smallest sink with only 3.6% (Fig. 26).

In summary, our study suggests that the relatively high $\delta^{15}\text{N}$ values of nitrate supplied by rivers are counteracted by atmospheric nitrogen with low $\delta^{15}\text{N}$ values. Moreover, a relatively enriched $\delta^{15}\text{N}$ signal “disappears” into the sediments which is different from other coastal seas, such as the German Bight (PÄTSCH et al. 2010). The next step is to further constrain the assumptions and to better understand the seasonal variability of nitrogen cycling in the Bohai and Yellow Sea.

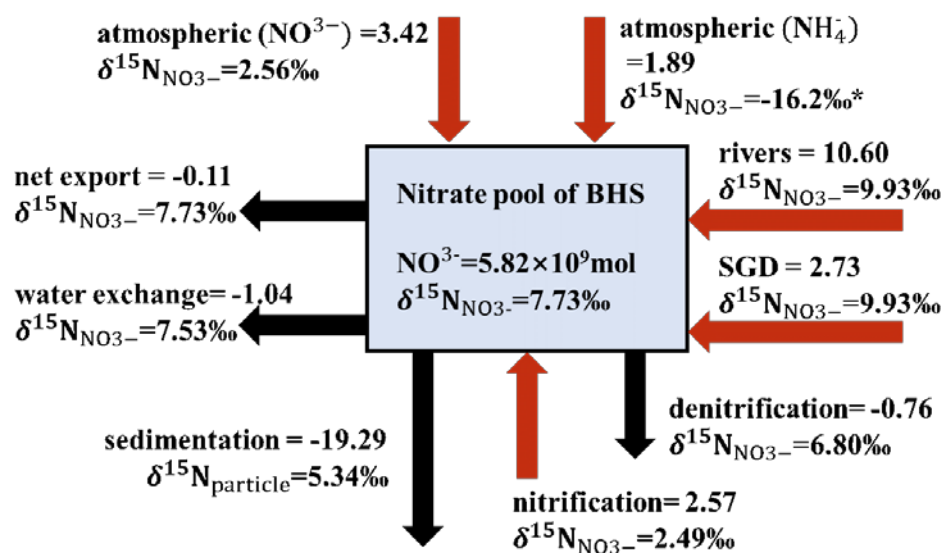


Fig. 26: Schematic diagram of the results of BHS nitrogen mass balance based on the isotope mass balance model using stable nitrogen isotopes of dissolved and particulate nitrogen from the BHS. The unit of nitrate is mol/yr if not indicated differently (*note: the $\delta^{15}\text{N}_{\text{NO}_3^-}$ is calculated assuming 30% oxidation of atmospheric NH_4^- inputs with corresponding $\delta^{15}\text{N}$).

Acknowledgements:

We thank the BMBF for funding the study in the Bohai and Yellow Seas and the PhD position of Shichao Tian within the project FINGNUTS (BMBF grant 03F0786B) as a subproject of the Sino-German research program MEGAPOL.

3.3 Environmental occurrence and distribution of selected current-used pesticides in the Chinese Bohai Sea and surrounding Rivers (Célia P.M. Bento³, Tanja Naumann³, Andreas Wittmann³, Jianhui Tang⁹, Xiaomei Zhen¹⁶ and Ralf Ebinghaus³)

Neonicotinoids (NNs), related insecticides and transformation products, as well as the herbicide glyphosate (GLY) are currently the most used pesticides worldwide (SIMON-DELISO et al. 2015, BENBROOK 2016). Their extensive use, the adverse effects of NNs to pollinators (SIMON-DELISO et al. 2015) and the probable links of GLY to cancer (IARC 2015) have put these compounds on the radar of society and policy makers. Consequently, they have emerged as environmental contaminants of concern.

This study investigates the occurrence and spatial distribution of 7 NNs (acetamiprid, clothianidin, dinotefuran, imidacloprid, nitenpyram, thiacloprid, thiamethoxam), fipronil (FIP), 3 new generation insecticides (imidaclothiz, (5S, 8R)-cycloxaprid, sulfoxaflor), GLY and several of their metabolites in the Chinese Bohai Sea and its surrounding rivers. In August 2018, 1 L (for insecticides) and 250 mL (for GLY and its main metabolite AMPA – aminomethylphosphonic acid) water samples were collected. In total, 47 stations in the Bohai Sea and 36 Bohai rivers were sampled. All samples were immediately stored at -20°C until analysis. For the insecticides, 1 L filtrated water samples were loaded onto Oasis HLB 500mg/6cc cartridges, eluted with 10 mL methanol (MeOH) and further enriched by evaporation, using an automated solid-phase extraction (SPE) and an EVAporation chamber (Freestyle Xana, LCTech, DE). For GLY&A, 20 mL of water were first derivatized with FMOC-Cl (9-Fluorenylmethoxycarbonyl chloride), followed by manual SPE. The derivatized samples were loaded onto Strata-X Polymeric Reversed Phase 200mg/6cc cartridges and eluted with 9 mL MeOH. All samples were analyzed by HPLC-MS/MS.

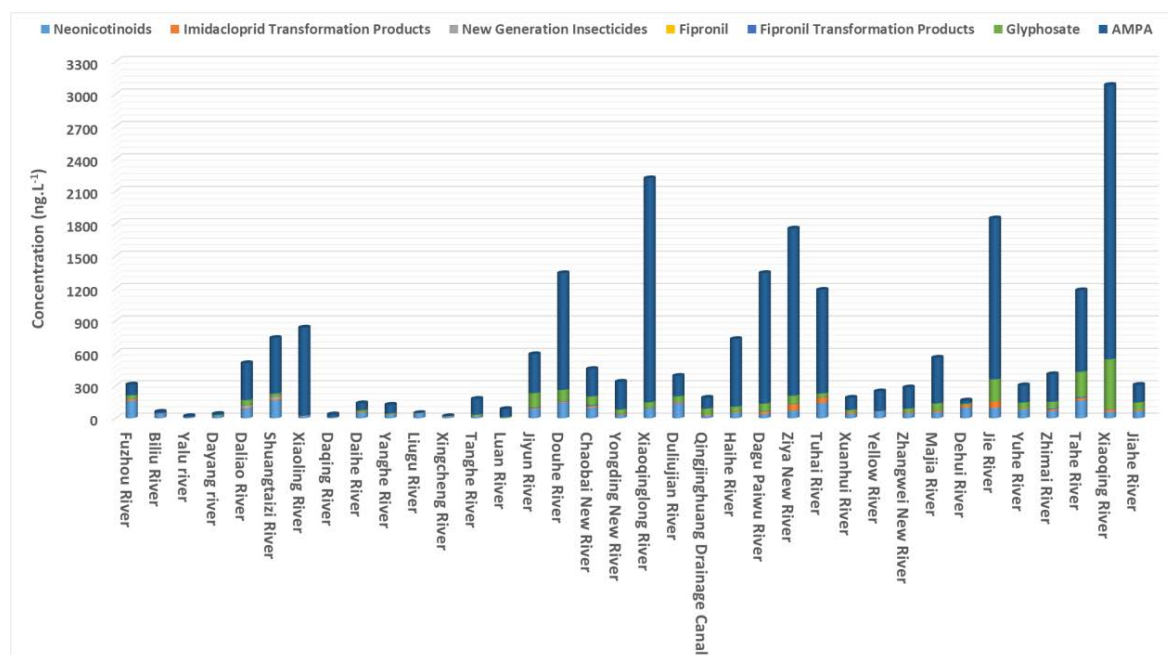


Fig. 27: Concentrations of elected Current-Used Pesticides (in ng L⁻¹) in 36 Rivers surrounding the Bohai Sea, in August 2018.

The results show that, from the 18 compounds analyzed, 15 were detected in River samples and 12 in seawater samples (Fig. 27, Fig. 28). Acetamiprid was detected in all river- and seawater samples, but imidacloprid, desnitro-imidacloprid and thiamethoxam were also detected in all river samples. Much higher concentrations were observed in the rivers ($\text{LOD} - 2538.6 \text{ ng L}^{-1}$) as compared to the Bohai Sea ($\text{LOD} - 120.5 \text{ ng L}^{-1}$). AMPA was the compound detected at the highest concentration for both river- (2538.6 ng L^{-1} – Xiaoqing River) and seawaters (120.5 ng L^{-1}), followed by glyphosate (Xiaoqing River = 463.6 ng L^{-1} ; seawater = 27.4 ng L^{-1}) and then by acetamiprid (Duliujian River = 127.4 ng L^{-1} ; seawater = 1.7 ng L^{-1}). New generation insecticides were not detected in all seawaters, whereas only imidacloprid was detected in 8% of the river samples.

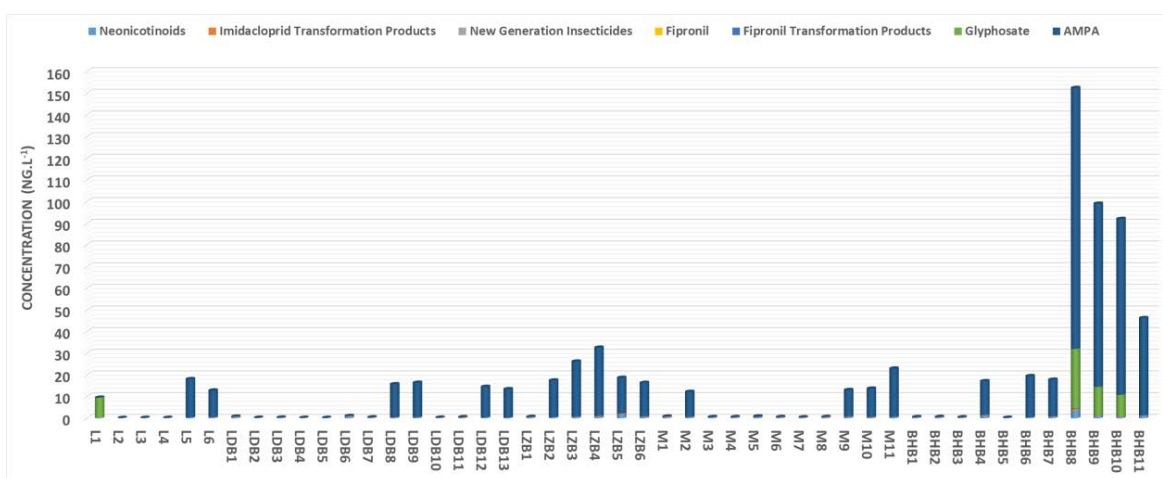


Fig. 28: Concentrations of Selected Current-Used Pesticides (in ng L^{-1}) in the Bohai Sea, in August 2018.

In conclusion, the ubiquitous presence of acetamiprid and the high concentrations and detection frequencies of AMPA in the sampled waters suggest that these compounds degrade slowly and may accumulate in aquatic/marine environments. All other compounds may pose a threat for riverine environments, but they seem to dissipate fast once they reach the Bohai Sea. The Bohai and Laizhou bays presented the highest contamination status, to where most contaminated rivers were flowing, indicating that riverine discharges are important contributors to the pollution status of the marine environment.

3.4 Halogenated flame retardants in the sediments of the Chinese Yellow Sea and East China Sea (Yanan Li^{10,14} and Jianhui Tang¹⁰)

Halogenated flame retardants (HFRs) are synthetic organic compounds that are commonly added to polymer materials to prevent ignition or inhibit flame propagation. These compounds are widely used in plastics, clothing, furniture, textiles, and electronics. Recently, China has become one of the largest consumers of flame retardants with an annual growth rate of HFR consumption as high as 7%, of which BFRs accounted for a large proportion (FINK et al. 2008). In 2013, HFRs comprised 31% of the global market for flame retardants (Flame retardants-online 2014).

With the phasing out of traditional polybrominated diphenyl ethers (PBDEs), significant volumes of alternative brominated flame retardants (aBFRs) are being used and released into the environment compartment, especially in coastal regions. In October 2017, during a research cruise campaign (R/V: Beidou), 38 surface sediment samples were collected from the YS and ECS. The levels and distribution of PBDEs, aBFRs, and dechlorane plus (DPs) were investigated in the surface sediments of the Yellow Sea (YS) and East China Sea (ECS) to examine the distribution and sources of these hydrophobic contaminants. The level and distribution of pollutants in the sediments of YS and ECS show obvious regional differences (see figure 2 in Li et al. 2019).

The Σ_7 PBDEs and BDE209 concentrations were 0.3–108.5 pg g⁻¹ dw and 1.1–924 pg g⁻¹ dw, with mean values of 20.4 and 127 pg g⁻¹ dw, respectively. The concentrations range of Σ_6 aBFRs and DBDPE were n.d. to 293 pg g⁻¹ dw (with a mean of 60.2 pg g⁻¹ dw) and n.d. to 9460 pg g⁻¹ dw (with a mean of 1700 pg g⁻¹ dw), respectively. As a major replacement for decabromodiphenyl ether (BDE 209), decabromodiphenyl ethane (DBDPE) was the dominant compound observed in the surface sediments, with a concentration one order of magnitude higher than that of BDE209. Furthermore, the trend of PBDEs consumption showed a slight decline, while the usage volume of aBFRs, especially for DBDPE, showed an increasing trend (see figure 2 in Li et al. 2019).

High concentrations were found in the depositional zones of the YS, indicating that these contaminants may originate from land-based pollution sources (likely from the Laizhou Bay manufacturing base) near the Bohai Sea. From inshore to offshore, the HFR concentrations showed a slightly increasing trend due to the presence of mud areas. The pollutants can be carried by the coastal current together with the sediment from the Yellow River, transported through the Bohai Strait and deposited in the mud zone of Northern and Southern YS (HU et al. 2011). Low levels of halogenated flame retardants (HFRs) were found in the estuary of the Yangtze River and ECS, indicating that Yangtze River contributes less HFRs to the region. Riverine discharge, atmospheric deposition, surface runoff, ocean current system, and mud area deposition effects may be significant factors influencing the distributions of HFRs. Moreover, the mud deposition zone on the shelf is likely the major sink of land-originated HFRs in the YS and ECS. With regards to the adverse effects of HFRs on organisms and the general environment, more measurements should be taken to monitor and control HFR pollution.

3.5 Legacy and novel halogenated flame retardants in seawater and atmosphere of the Bohai Sea, China (Lin Liu^{16,9,14}, Xiaomei Zhen^{16,9,14}, Xinming Wang¹⁶, Yanfang Li^{9,15}, Xu Sun^{9,14} and Jianhui Tang^{9,15})

China is one of the largest flame retardant producers and users in the world, and Laizhou Bay area is the biggest production base for brominated flame retardants (BFRs) (ZHEN et al. 2018).

The environmental fates of HFRs, particularly nHFRs, in the seawater and atmosphere of the Bohai Sea are not well understood. In this study, HFR concentrations were measured in seawater and air in August and December 2016, and February and June 2017, in the Bohai Sea. This is the first study to present the concentration levels and spatial distributions of HFRs across the whole area. Overall, 29 seawater and 27 air samples were collected during four time periods to investigate the seasonal variation of HFRs and explore the influential factors and potential HFR sources in the Bohai Sea.

In conclusion, BDE209 and DBDPE were dominant compounds in this study, which were prone to be partitioned to the particle phase. Although Deca-BDE technical mixture should be gradual phasing out due to the prohibition globally, there are still a lot of residues of BDE209, and even some production sources in environment of the Bohai Rim according to our study. The alternative, DBDPE, has quickly dominated in the environment (see figure 1 in LIU et al. 2020). In some shallow ocean regions where were not directly affected by production emissions, resuspension from sediment and delayed transfer by ocean currents could result in the redistribution of contaminants. Therefore, in the study of offshore contaminations, hydrodynamic factors cannot be ignored, and the data collected over a short period are insufficient to allow for an accurate ecosystem risk assessment of pollutants.

No notable seasonality was found for HFRs in the atmosphere, but the high concentration in winter was usually accompanied by high values of total suspended particles (TSP; see figure 1 in LIU et al. 2020), which could carry contaminations that were easily partitioned to the particulate phase and aggravate air pollution in winter. The estimated atmospheric deposition fluxes of HFRs were 19, 51, and 80 kg season⁻¹ in spring, summer, and winter, respectively, indicating an important role of atmospheric fluxes of HFRs to the ocean as a component of the marine organic carbon budget. These massive inputs of BDE209 and DBDPE in the largest production area of north China will have an important and profound biogeochemical implication in the future.

Acknowledgements:

This study was supported by the National Science Foundation of China (No. 41773138 and U1806207), the seed project of the Yantai Institute of Coastal Zone Research, Chinese Academy of Sciences (No. YIC Y855011024) and the Chinese Academy of Sciences (XDA11020402).

3.6 Identification of elements distribution patterns in the delta-estuary region by a combined magnetic and isotopic approach (Yuan Li⁹ and Yongming Luo^{9,10})

Environmental magnetism and isotope techniques are robust tools that have been successfully used to elucidate distribution patterns, sources, mixing and transformations of metals, carbon and nitrogen in the terrestrial, estuarine and coastal regions. Our studies (Li et al. 2018, Li et al. 2016) attempt to characterize the red clay-yellow silt sequence and fluvial

sediments in the Yellow River Delta (YRD) and its adjacent estuaries using these two techniques, and to provide insights into the changes of metals and nutrients in relationship with the transportation and deposition process, aiming to provide a better understanding of processes that control the environmental changes in the coastal zone.

The results showed that the red clay layer (RCL) in the YRD soil profiles had unique magnetic properties. The magnetic enhancement of the RCL could be attributed to the presence of fine superparamagnetic (SP)/single domain (SD) ferrimagnetic grains sourcing from hydrodynamic sorting of old sediments (e.g., paleosol in the Chinese Loess Plateau). Three units were identified in a high resolution soil profile based on the changes of magnetic curves, including a steady deposition process in the upper unit, a strong hydrodynamic process with varied provenance in the middle unit and a heterogeneous deposition process in the lower unit with the RCL (Fig. 29).

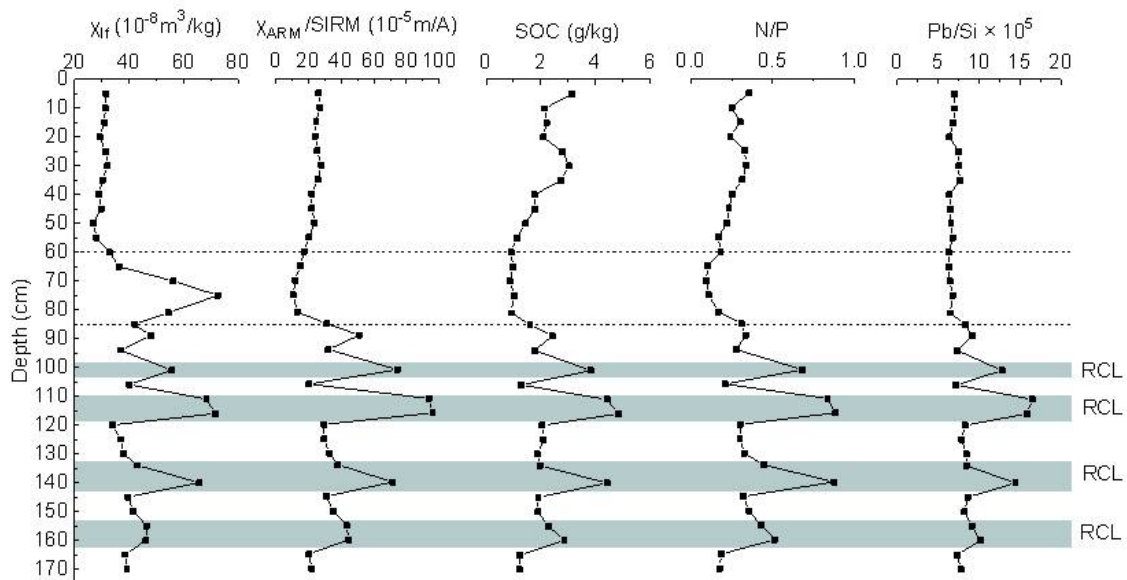


Fig. 29: An example showing depth distributions of magnetic properties and elements in the RCL-YSL sequence of the Yellow River Delta.

The three units were closely linked to the variation of nutrients (carbon and nitrogen) and metals (chromium (Cr), copper (Cu), nickel (Ni), lead (Pb), zinc (Zn), titanium (Ti) and zirconium (Zr)) in the soil profile, indicating the influence of provenance and sorting during sediment transportation and deposition. The magnetic method is sensitive to characterize soil formation and environmental changes in the coastal zone.

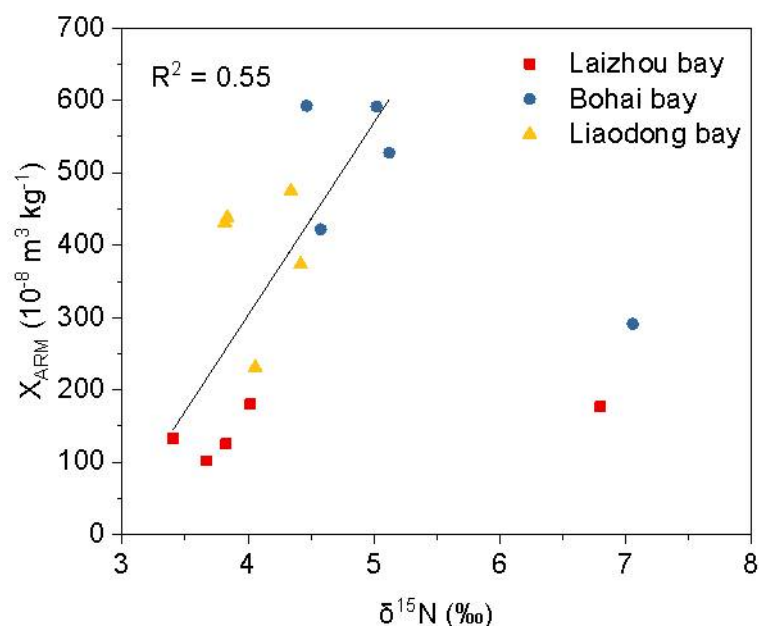


Fig. 30: Correlation between anhyseretic remanent magnetization (χ_{ARM}) and $\delta^{15}\text{N}$ values in bed sediments of estuarine mixing zone from the Laizhou Bay, Bohai Bay and Liaodong Bay of the Bohai Sea.

It was notable that although RCL had highest weathering intensity as indicated by highest $\chi_{\text{fd}}\%$ values, the average $\Delta^{14}\text{C}$ value of the RCL was much higher than that of the YSL and YR, indicating that the RCL received more younger OC. A spatial heterogeneity of both $\delta^{13}\text{C}$ and $\delta^{15}\text{N}$ values were observed in the Yellow River plume and its adjacent bay areas, indicating that Yellow River sediment transport and anthropogenic wastewater discharge were two driving forces for the sedimentary organic carbon and nitrogen dynamics in large river plume and inner bay areas. Recently, our preliminary results showed a significantly positively correlation between $\delta^{15}\text{N}$ values and magnetic indicators (e.g., χ_{ARM}) in the bed sediments of estuaries in the Bohai sea (Fig. 30). This indicates that the elevated $\delta^{15}\text{N}$ values may be related to the input of highly-weathered fine sediments from the basin to the sea.

Acknowledgements:

Portions of these works were funded by the National Natural Science Foundation of China and the Sino–German Joint Project on Marine and Polar Cooperation.

4 Comparison of the European and Asian marginal seas

In this chapter, we compare the different hydrographic systems of the Pearl River Estuary-South China Sea and the much more northerly Yangtze River-Bohai Sea-Yellow Sea system with the temperate Baltic and North Seas in terms of the fate of modern pollutants in coastal seas. We focus on the "Four Seas" not only because we are familiar with these seas after many years of scientific analysis, but also because of their societal importance with a wide range of important ecosystem services. These systems consist of one sea that is more enclosed and another that is semi-open to the world ocean. Both systems are home to important ecosystems, with the difference that the northern European seas have many different national coasts, while in the case of the Chinese seas, only a limited number of international partners share responsibility for the marginal seas.

4.1 Occurrence and risk of organic UV absorbers in marine sediments of Europe and China (Andreas Wittmann³, Christina Apel^{3,6}, Jianhui Tang⁹ and Ralf Ebinghaus³)

While initially the research on UV-absorbing compounds (UVAs) in the late 1990's and early 2000's was focused on freshwater ecosystems, recent studies emphasize the presence of UVAs in the marine and coastal environment. The widespread use of UV stabilizers in plastics and the use of UV filters in personal care products (PCPs) combined with their high production volumes, an incomplete elimination in wastewater treatment and a relative stability against degradation, leads to persistent or "pseudo-persistent" characteristics in the environment and their ubiquitous detection across environmental compartments. Additionally, several studies have shown the potential of select UVAs to accumulate in aquatic organisms and to affect their hormonal system (endocrine disruption). This has given rise to increasing concern about the environmental safety and potential risks of these environmental contaminants.

In the light of a growing global population and the progressing trends of urbanization, industrialization and global tourism, a continued, strong demand for consumer products that contain UVAs can be expected. An increase in the discharge of UVAs will likely be the consequence. Following these trends, UV filters and UV stabilizers will remain an important research topic, when estimating and assessing the pollution footprint of big cities on their surrounding environment. In order to develop effective solutions for risk reduction and prevention, it is important to know more about the occurrence, distribution and the environmental fate of these compounds, as well as their toxicological potential.

Due to comparatively high LogK_{ow} values, many UVAs tend to sorb to organic matter. Sediment is therefore a likely sink. Studies on UVAs in marine sediments are scarce and detailed data on their occurrence and distribution is still lacking. To serve this research need, we developed a PLE-HPLC-MS/MS method (Apel et al. 2018a), capable of determining 22 UVAs in marine sediments. 74 surface sediment samples from the Chinese Bohai and Yellow Seas as well as 56 samples from the European North and Baltic Seas were analyzed. With a concentration range of <MQL to 26 ng/g dw (Σ UVAs) and an average concentration of 2 ng/g dw (Σ UVAs), Chinese sediments were only slightly more polluted than the samples from the

European marine environment (<MDL to 11.2 ng/g dw, avg. conc.: 1.2 ng/g) (Fig. 31, please also see figure 2 in APEL et al. 2018a and figure 1 in APEL et al. 2018b). In both cases, octocrylene was the UVA with the highest concentrations and clearly dominated the distribution (APEL et al. 2018a, APEL et al. 2018b). A comparison of the UVA distribution revealed region and emission specific patterns. Finally, for six compounds a preliminary hazard quotient was calculated. Based on the scarce toxicity data available for marine organisms, an immediate risk for benthic organisms in the study area was not revealed.

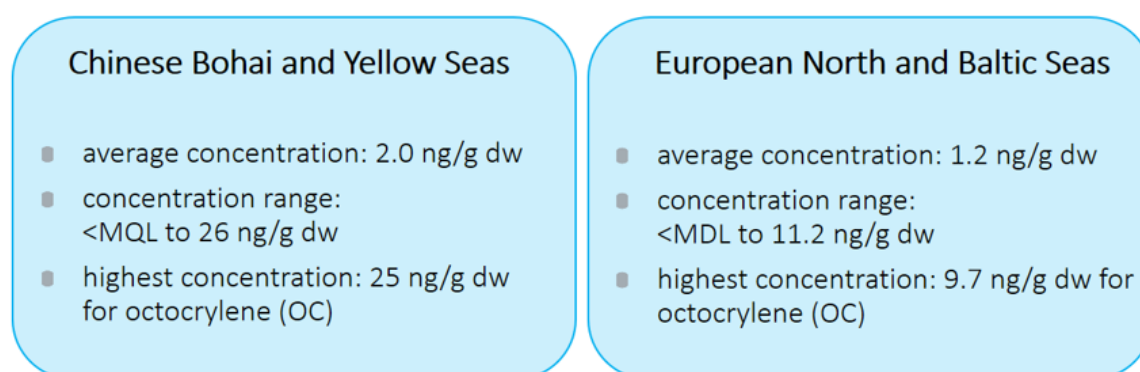


Fig. 31: Comparison of the UVA concentrations in Chinese and European sediments.

4.2 Emerging and novel per- and polyfluoroalkyl substances in Chinese and German river water impacted by point sources (Hanna Joerss³, Jianhui Tang⁹, Thekla-Regine Schramm³, Linting Sun⁹, Chao Guo⁹, Frank Menger⁵, Lutz Ahrens⁵ and Ralf Ebinghaus³)

Per- and polyfluoroalkyl substances (PFASs) are a group of man-made chemicals that have been produced and used for over 60 years due to their unique water- and oil-repellent properties along with their high stability (KISSA 2001). Since the late 1990s, attention has been drawn to their role as global contaminants because several long-chain PFASs have been shown to be persistent, bioaccumulative, toxic, and ubiquitously present in the environment (KRAFFT & RIESS 2015). A new global database lists 4730 PFAS-related CAS numbers, which are on the worldwide market (OECD 2018). Using conventional compound-specific analytical methods, only a small fraction of the PFASs on the global market can be determined. Thus, there is a knowledge gap if the currently monitored PFASs are representative or only make up a small fraction of anthropogenic PFAS releases.

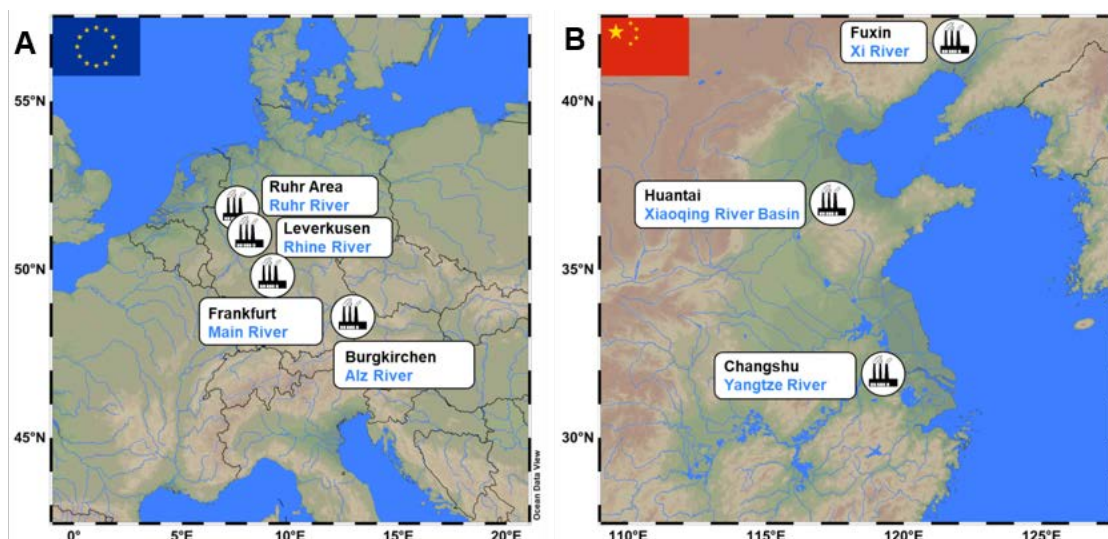


Fig. 32: Location of the A) German and B) Chinese manufacturing sites close to which river samples were taken. At each site, samples were taken at 7-8 sampling locations, up- and downstream the potential source (JOERSS et al. 2020).

The aim of this study was to investigate the occurrence and distribution of emerging and novel PFASs in river water taken close to industrial point sources in Europe and China (Fig. 32A, B). Moreover, the study aimed at characterizing the unknown pool of PFASs by using the Total Oxidizable Precursor (TOP) assay and high resolution mass spectrometry (HRMS)-based methods.

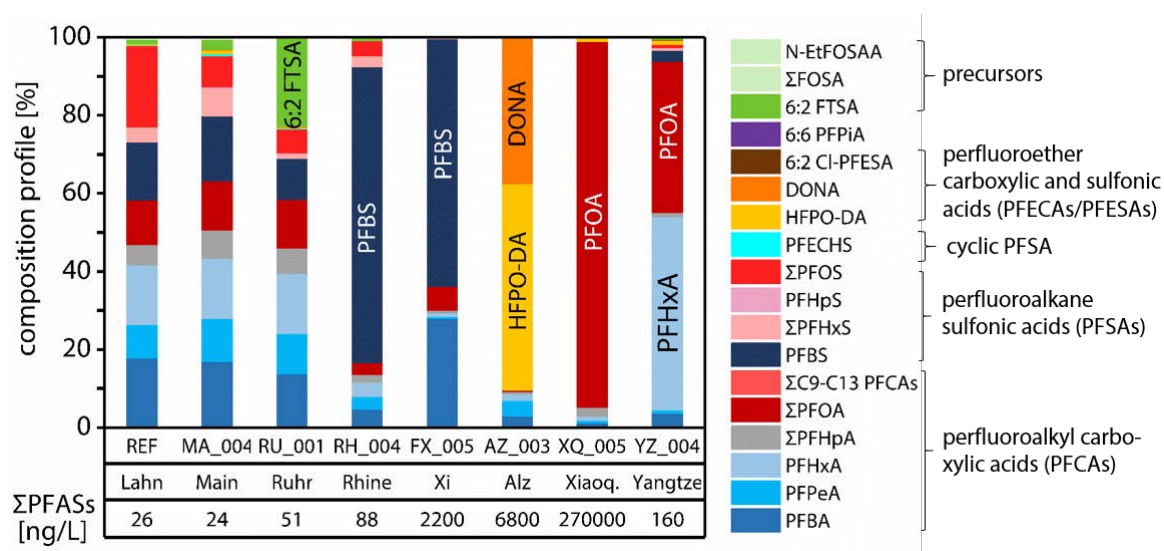


Fig. 33: Source-specific PFAS patterns and Σ PFASs [ng/L] in selected samples, analysed by LC-MS/MS (JOERSS et al. 2020).

The sum of PFASs analysed by liquid chromatography-tandem mass spectrometry (LC-MS/MS) varied between 2.7 ng/L in the German Alz River and 420,000 ng/L in the Chinese Xiaoqing River Basin. Moreover, source- and country-specific patterns could be identified. The well-known legacy compound perfluorooctanoate (PFOA) was the most prevalent substance near a Chinese fluoropolymer manufacturing site, contributing to Σ PFASs with about 90%. On

the other hand, the per- and polyfluoroether carboxylates HFPO-DA and DONA, which are replacement compounds of PFOA, were the predominant PFASs close to a German fluoropolymer production facility, contributing to ΣPFASs with about 50% and 40% (Fig. 33). In contrast, the perfluoroether sulfonate 6:2 Cl-PFESA, a replacement compound for perfluorooctane sulfonate (PFOS), was more frequently detected in China (JOERSS et al. 2020).

Using the TOP assay as a parameter for estimating total PFASs (HOUTZ & SEDLAK 2012), the molar concentration of perfluoroalkyl carboxylates (PFCAs) increased significantly after sample oxidation. This indicated the presence of a fraction of unknown PFAS precursors. To characterize the composition of the latter, a HRMS-based suspect screening approach was used. It revealed several PFAS homologue series and new individual PFASs that were not included in the LC-MS/MS target method.

The results show that conventional target analysis of known PFASs only accounts for a small fraction of the PFASs present in Chinese and German river water impacted by point sources. Consequently, environmental and human exposure to PFASs may be underestimated. The use of complementary methods, such as the TOP assay and HRMS-based approaches, provides a more comprehensive understanding of PFAS composition, sources and potential risks.

4.3 Spatial distribution of microplastics: comparison between the Bohai and Baltic seas (Qian Zhou⁹, Chuancheng Fu^{9,10}, Jie Yang¹⁰, Kuanxu Xiong⁹, Yuan Li⁹, Chen Tu⁹, Lianzhen Li⁹, Yongming Luo^{9,10} and Joanna J. Waniek⁴)

The occurrence of and risks from microplastics in coastal seas are of increasing global concern. Several studies report that microplastics were more likely to accumulate in semi-enclosed coastal seas. Here, we investigate the vertical distribution and composition of microplastics in the Bohai and Baltic seas. Water samples were collected from different depths of the water column within 63 m in the Bohai Sea and within 437 m in the Baltic Sea. The average vertical abundance of microplastics in the Bohai Sea was 6.11 ± 7.2 items L^{-1} , slightly higher than in the Baltic (5.8 ± 5.0 items L^{-1}). Microplastics in the Bohai Sea accumulated mainly in the surface waters. This may be due to strong surface flow under the control of the winter winds inhibiting the downward migration of particles (CORCORAN 2015, LI et al. 2015). However, microplastics in the Baltic Sea accumulated mostly in the halocline layers, possible due to a large change in density resulting from the input of high salinity seawater from the North Sea (BAGAEV et al. 2017). Both seas had fibers, fragments and films, but pellets were found only in the Bohai Sea. Seven microplastic polymers, namely polyethylene, polypropylene, polyester, rayon, poly (vinyl acetate), polyvinyl chloride and copolymer, were identified in the Bohai Sea. The Baltic showed slight differences in the composition of microplastic polymers comprising polyethylene, polypropylene, polyester, rayon, polyvinyl chloride, polyamide, polytetrafluoroethylene and polybutene. Fibers were the most abundant microplastics in both the Bohai (92.4%) and the Baltic (90.6%). There was much more rayon in the Baltic (87.2%) than in the Bohai (37.5%). The microplastic particles

in the Baltic were smaller on average than those in the Bohai Sea. The number of microplastics < 1 mm accounted for 54.6% in the Bohai and 77.5% in the Baltic. In summary, the vertical distribution of microplastics was controlled mainly by the hydrodynamics in the Bohai Sea but was strongly influenced by seawater density in the Baltic. Moreover, differences in the abundance and composition of microplastic polymers in both seas were also influenced by human activities along the local coastal zones (DAI et al. 2018, HENGSTMANN et al. 2018).

Acknowledgements:

This work was funded by the National Key Research and Development Program of China (Grant No. 2016YFC1402202), the Sino-German MEGAPOL consortium (BMBF, Contract No. 03Fo786A), the Key Research Program of Frontier Sciences, CAS (Grant No. QYZDJ-SSW-DQCo15), and the External Cooperation Program of BIC, Chinese Academy of Sciences (Grant No. 133337KYSB20160003). The English was revised by Prof. Peter Christie, Institute of Soil Science, Chinese Academy of Sciences, Nanjing, China.

4.4 Characterization of biofilms formed on the surface of diverse types of microplastics in the seawater of the Baltic Sea (Chen Tu^{9,1}, Qian Zhou^{9,1}, Ying Liu⁹, Xinning Zhang⁹, Joanna J. Waniek¹ and Yongming Luo^{9,10})

The effects of microbial colonization and biofilm formation on microplastics (MPs) in the marine environments are of growing global concern (ZHOU et al. 2020). The biofilm formation may affect the physical and chemical properties of the MPs, such as surface micro-morphology and roughness, surface charge, specific surface area, and density, and may also affect the microbial community structure and diversity in the ambient environment [2]. In this study, three different types of MPs, polyethylene (PE) films, polypropylene (PP) pallets and expanded polystyrene (EPS) foams were immersed in a tank filled with seawater from the Baltic Sea for 30 days with a sampling interval of 10 days. The aim of this study was to illustrate the dynamic characterization of biofilm formation on the surfaces of the different MPs.

The total amount (biomass) of biofilms formed on the MPs surfaces was quantitatively determined by crystal violet staining. The results show that the biofilm biomass formed on the surface of all 3 types of the MPs increased with time. This was consistent with previous study which demonstrated that the biofilm formation in offshore environments happens within a few hours, and could last for several months or even longer (TU et al. 2020).

The morphology of the biofilms on the surfaces of the MPs was observed by scanning electron microscopy (SEM). A variety of biofilm morphological types were observed on the surface of PE, PP and EPS, including rod shaped bacterial cells, intertwined filaments, diatoms, as well as a dense layer of extracellular polymeric substances (Fig. 34).

High-throughput DNA sequencing was used to compare the dynamic shifting of microbial communities that colonized the surfaces of the different MPs with the ambient seawater. The community heat map for MPs biofilms and seawater was drawn on Phylum level. The PE associated biofilms showed significantly different microbial community profiles in comparison to the PP and the EPS associated biofilms. Moreover, all the MPs associated biofilms exhibited a significantly distinct microbial community structure in comparison to those from the seawater. This indicated that MPs, as a new marine microbial habitat, can provide a novel niche for the marine microbes, and the selective colonization and formation of biofilms by marine microbes on MPs surfaces may be further affected by the polymer types of MPs.

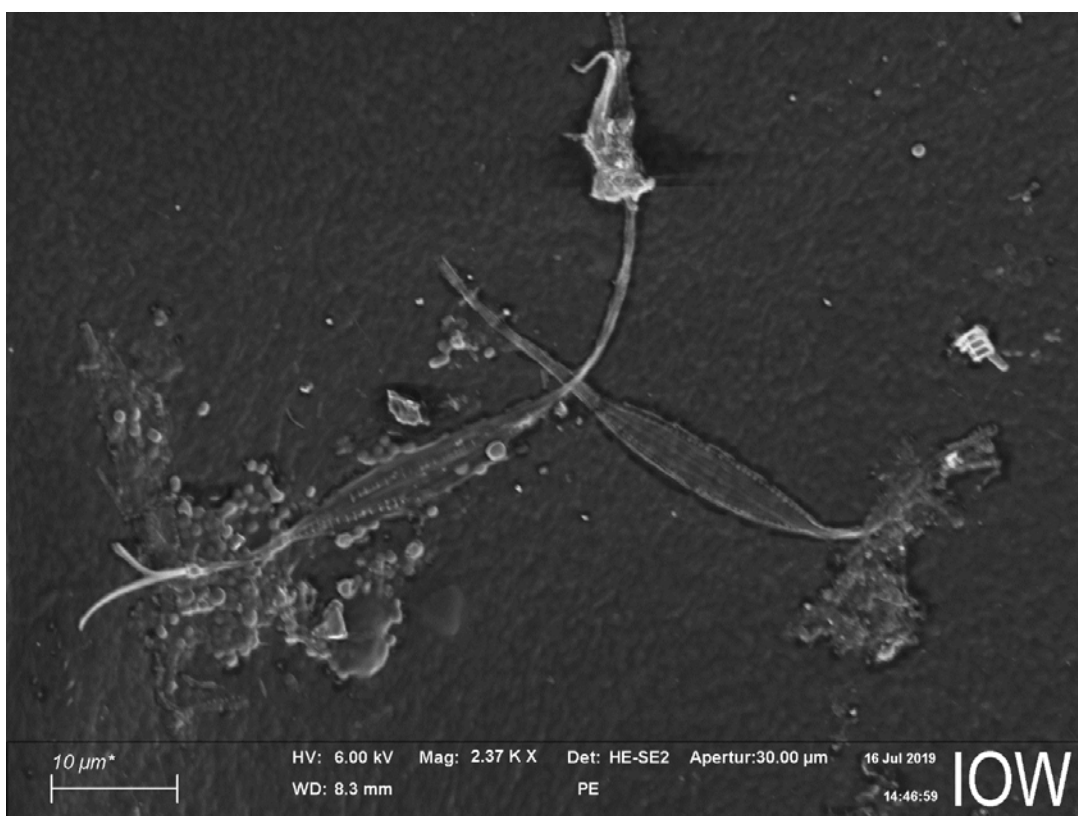


Fig. 34: SEM image of the biofilm formed on the surface of PE.

Acknowledgements:

This work was funded by the Key Research Program of Frontier Sciences, CAS, China (No. QYZDJSSW-DQCo15), and the Sino-German International Cooperation Project, BMBF, Germany (No. 03Fo786A).

5 Conclusions and outlook

We believe that our successful and sustained collaboration between the German and Chinese coastal researcher institutions involved in MEGAPOL holds the potential for significant progress in marine science, especially on the coastal regions. We expect synergistic progress in terms of an improved understanding of involved processes at the system and subsystem level, the holistic system of natural dynamics and human influence, and perspectives conditioned by different societal values and preferences, while looking at the two North German marginal seas of the North Sea and the Baltic Sea as well as the Chinese marginal seas in parallel and especially in a comparative way.

We do hope that our successful cooperation within the bilateral Sino-German MEGAPOL joint network will continue in the future in the framework of a different project. Until then we certainly will be working on joint publications, developing new ideas and keeping our friendship alive. In that way the concept of the “Four Seas” will be kept alive, and might be open up to investigations in other European and Asian marginal seas.

Acknowledgements

With the end of this successful joint bilateral project it is time to thank all involved person on land and at sea for their help and support. We thank the numerous student helpers, technicians and scientists for their work as well as the administrations of all involved institutes as well as the crews of the Chinese and German research vessels we have used for our expeditions. We acknowledge as well the funding from the BMBF on the German side (grant numbers 03Fo786A–C (MEGAPOL), 03Go269A–B (SOCLIS) and 01DO17038 (TRAN)) and from SOA on the Chinese side.

References

- APEL, C., JOERSS, H., EBINGHAUS, R. 2018a: Environmental occurrence and hazard of organic UV stabilizers and UV filters in the sediment of European North and Baltic Seas. *Chemosphere* **212**, 254–261.
- APEL, C., TANG, J., EBINGHAUS, R., 2018b: Environmental occurrence and distribution of organic UV stabilizers and UV filters in the sediment of Chinese Bohai and Yellow Seas. *Environmental Pollution*, **235**, 85–94.
- BAGAEV, A., MIZYUK, A., KHATMULLINA, L., ISACHENKO, I., CHUBARENKO, I., 2017: Anthropogenic fibres in the Baltic Sea water column: Field data, laboratory and numerical testing of their motion. *Science of the Total Environment*, **599**, 560–571.
- BENBROOK, C. M., 2016: Trends in glyphosate herbicide use in the United States and globally. *Environmental Sciences Europe*, **28**, p. 3.
- CASCIOTTI, K. L., 2016: Nitrogen and Oxygen Isotopic Studies of the Marine Nitrogen Cycle. *Annual Review of Marine Science*, **8**, 379–407.
- CASSAR, N., BARNETT, B. A., BENDER, M. L., KAISER, J., HAMME, R. C., TILBROOK, B., 2009: Continuous high-frequency dissolved O₂/Ar measurements by equilibrator inlet mass spectrometry. *Analytical Chemistry*, **81**(5), 1855–64.
- CHEN, J., NI, X., LIU, M., CHEN, J., MAO, Z., JIN, H., PAN, D. 2014: Monitoring the occurrence of seasonal low oxygen events off the Changjiang Estuary through integration of remote sensing, buoy observations, and modelling. *Journal of Geophysical Research: Oceans*, **119**(8), 5311–5322.
- CHEN, Y.-L. L., CHEN, H.-Y., LIN, Y.-H., 2003: Distribution and downward flux of Trichodesmium in the South China Sea as influenced by the transport from the Kuroshio current. *Marine Ecology Progress Series*, **259**, 47–57.
- CORCORAN, P. L., 2015: Benthic plastic debris in marine and fresh water environments. *Environmental Science: Processes and Impacts*, **17**(8), 1363–1369.
- DAI, Z., ZHANG, H., ZHOU, Q., TIAN, Y., CHEN, T., TU, C., FU, C., LUO, Y., 2018: Occurrence of microplastics in the water column and sediment in an inland sea affected by intensive anthropogenic activities. *Environmental Pollution*, **242**, 1557–1565.
- DIAZ R.J., ROSENBERG R., 2008: Spreading Dead Zones and Consequences for Marine Ecosystems. *Science*, **321**, 926–929.
- FINK, U., HAJDUK, F., WEI, Y., & MORI, H., 2008: Flame Retardants. (S. Consulting, Hrsg.) online available: <http://www.flameretardants-online.com/web/en/106/114.htm>.
- FISCH, K., ZHANG, R., ZHOU, M., SCHULZ-BULL, D. E., WANIEK, J. J. (2021): PPCPs – A human and veterinary fingerprint in the Pearl River Delta and the northern South China Sea. *Emerging Contaminants*, **7**, 10–21.

- GAYE, B., NAGEL, B., DÄHNKE, K., RIXEN, T., LAHAJNAR, N., EMEIS, K.-C., 2013: Amino acid composition and $\delta^{15}\text{N}$ of suspended matter in the Arabian Sea: implications for organic matter sources and degradation. *Biogeosciences*, **10**, 7689–7702.
- GAYE, B., WIESNER, M. G., LAHAJNAR, N., 2009: Nitrogen sources in the South China Sea, as discerned from stable nitrogen isotopic ratios in rivers, sinking particles, and sediments. *Marine Chemistry*, **114**(3–4), 72–85.
- HENGSTMANN, E., TAMMINGA, M., VOM BRUCH, C., FISCHER, E. K., 2018: Microplastic in beach sediments of the Isle of Rügen (Baltic Sea): Implementing a novel glass elutriation column. *Marine Pollution Bulletin*, **126**, 263–274.
- HERMAN, A. W., 1983: Vertical distribution patterns of copepods, chlorophyll, and production in northeastern Baffin Bay. *Limnology and Oceanography*, **28**(4), 709–719.
- HERMAN, A. W., BEANLANDS, B., PHILLIPS, E. F., 2004: The next generation of Optical Plankton Counter: the Laser-OPC. *Journal of Plankton Research*, **26**(10), 1135–1145.
- HOUTZ, E. F., SEDLAK, D. L., 2012: Oxidative conversion as a means of detecting precursors to perfluoroalkyl acids in urban runoff. *Environmental Science & Technology*, **46**(17), 9342–9349.
- HU, L. M., LIN, T., SHI, X. F., YANG, Z. S., WANG, H. J., ZHANG, G., GUO, Z. G., 2011: The role of shelf mud depositional process and large river input on the fate of organochlorine pesticides in sediments of the Yellow and East China seas. *Geophysical Research Letters*, **38**(3), L03602.
- IARC, 2015: IARC monographs on the evaluation of carcinogenic risks to humans, volume 112: Some organophosphate insecticides and herbicides/ IARC Working Group on the Evaluation of Carcinogenic Risks to Humans. Lyon, France, 464pp.
- IPCC, 2007: Climate Change 2007: Synthesis Report. Contribution of Working Groups I, II and III to the Fourth Assessment Report of the Intergovernmental Panel on Climate Change [Core Writing Team, Pachauri, R.K. and Reisinger, A. (eds.)]. IPCC, Geneva, Switzerland, 104pp.
- JIA, G., PENG, P., 2003: Temporal and spatial variations in signatures of sedimented organic matter in Lingding Bay (Pearl estuary), southern China. *Marine Chemistry*, **82**, 47–54.
- JOERSS, H., SCHRAMM, T.-R., SUN, L., GUO, C., TANG, J., EBINGHAUS, R., 2020: Per- and polyfluoroalkyl substances in Chinese and German river water – Point source- and country-specific fingerprints including unknown precursors. *Environmental Pollution*, **267**, 115567.
- KAISER, D., SCHULZ-BULL, D. E., WANIEK, J. J., 2018: Polycyclic and organochlorine hydrocarbons in sediments of the northern South China Sea. *Marine Pollution Bulletin*, **137**, 668–676.
- KENDALL, C., ELLIOTT, E. M., WANKEL, S. D., 2007: Tracing anthropogenic inputs of nitrogen to ecosystems. In R. Michener, & K. Lajtha (Eds.), *Stable Isotopes in Ecology and Environmental Science*. Blackwell Publishing.

- KISSA, E., 2001: Fluorinated Surfactants and Repellents (2nd edition Aug.). New York: Marcel Dekker.
- KOMEN, G. J., CAVALERI, L., DONELAND, M., HASSELMANN, K., HASSELMANN, S., & JANSSEN, P. A., 1994: Dynamics and modelling of ocean waves. Cambridge University Press, UK, 550pp.
- KRAFFT, M. P., RIESS, J. G. 2015: Per- and polyfluorinated substances (PFASs): Environmental challenges. *Current Opinion in Colloid & Interface Science*, **20**(3), 192–212.
- LAFFOLEY, B., BAXTER, J. M., 2019: Ocean deoxygenation: Everyone's problem - Causes, impacts, consequences and solutions. Gland, Switzerland: IUCN.
- LI, J., SONG, J., MU, L., WANG, Y., LI, Y., WANG, G., 2015: Characteristics of seawater exchange in the Bohai sea and the Yellow sea under the influence of winter winds. *Haiyang Tongbao*, **34**(6), 647–656 (in Chinese).
- LI, K. Z., YIN, J. Q., HUANG, L. M., TAN, Y. H., 2006: Spatial and temporal variations of mesozooplankton in the Pearl River estuary, China. *Estuarine Coastal and Shelf Science*, **67**, 543–552.
- LI, X., LU, C., ZHANG, Y., ZHAO, H., WANG, J., LIU, H., YIN, K., 2020: Low dissolved oxygen in the Pearl River estuary in summer: Long-term spatio-temporal patterns, trends, and regulating factors. *Marine Pollution Bulletin*, **151**, 110814.
- LI X., BIANCHI, T. S., YANG, Z., OSTERMAN, L. E., ALLISON, M. A., DIMARCO, S. F., YANG, G., 2011: Historical trends of hypoxia in Changjiang River estuary: Applications of chemical biomarkers and microfossils. *Journal of Marine Systems*, **86**(3–4), 57–68.
- LI, Y., ZHANG, H., TU, C., LUO, Y., 2018: Magnetic characterization of distinct soil layers and its implications for environmental changes in the coastal soils from the Yellow River Delta. *Catena*, **162**, 245–254.
- LI, Y., ZHANG, H., TU, C., FU, C., XUE, Y., LUO, Y., 2016: Sources and fate of organic carbon and nitrogen from land to ocean: Identified by coupling stable isotopes with C/N ratio. *Estuarine, Coastal and Shelf Science*, **181**, 114–122.
- LI, Y., ZHEN, X., LIU, L., TIAN, C., PAN, X., TANG, J., 2019: Halogenated flame retardants in the sediments of the Chinese Yellow Sea and East China Sea, *Chemosphere*, **234**, 365–372.
- LIU, L., ZHEN, X., WANG, X., LI, Y., SUN, X., TANG, J., 2020: Legacy and novel halogenated flame retardants in seawater and atmosphere of the Bohai Sea: Spatial trends, seasonal variations, and influencing factors. *Water Research*, **184**, 116117.
- LIU, S. M., HONG, G.-H., ZHANG, J., YE, X. W., JIANG, X. L., 2009: Nutrient budgets for large Chinese estuaries. *Biogeosciences*, **6**, 2245–2263.
- LIU, S. M., LI, L. W., ZHANG, Z., 2011: Inventory of nutrients in the Bohai. *Continental Shelf Research*, **31**, 1790–1797.
- LIU, S. M., ZHANG, J., JIANG, W. S., 2003: Pore water nutrient regeneration in shallow coastal Bohai Sea, China. *Journal of oceanography*, **59**, 377–385.

- LIU, Y. L., GAO, S., WANG, Y. P., YANG, Y., LONG, J. P., ZHANG, Y. Z., WU, X. D., 2014: Distal mud deposits associated with the Pearl River over the northwestern continental shelf of the South China Sea. *Marine Geology*, **347**, 43–57.
- LÜDMANN, WONG, H. K., WANG, P., 2001: Plio–Quaternary sedimentation processes and neotectonics of the northern continental margin of the South China Sea. *Marine Geology*, **172**, 331–358.
- MORTHORST, J. E., BRANDE-LAVRIDSEN, N., KORSGAARD, B., BJERREGAARD, P., 2014: 17 β -Estradiol Causes Abnormal Development in Embryos of the Viviparous Eelpout. *Environmental Science & Technology*, **48**(24), 14668–14676.
- MULLER-KARGER, F. E., 2005: The importance of continental margins in the global carbon cycle. *Geophysical Research Letters*, **32**, L01602.
- NING, X., LIN, C., SU, J., LIU, C., HAO, Q., LE, F., TANG, Q., 2010: Long-term environmental changes and the responses of the ecosystems in the Bohai Sea during 1960–1996. *Deep Sea Research Part II: Topical Studies in Oceanography*, **57**, 1079–1091.
- OECD, 2018: Toward a new comprehensive global database of per- and polyfluoroalkyl substances (PFASs): Summary report on updating the OECD 2007 list of per- and polyfluoroalkyl substances (PFASs). Series on Risk Management No. 39, Organisation for Economic Co-operation and Development (OECD).
- OHNO, T., 2002: Fluorescence inner-filtering correction for determining the humification index of dissolved organic matter. *Environmental Science & Technology*, **36**(4), 742–746.
- OU, S., ZHANG, H., WANG, D.-X., HE, J., 2007: Horizontal Characteristics of Buoyant Plume off the Pearl River Estuary during Summer. *Journal of Coastal Research*, SI 50 (Proceedings of the 9th International Coastal Symposium), 652–657.
- PÄTSCH, J., SERNA, A., DÄHNKE, K., SCHLARBAUM, T., JOHANNSEN, A., EMEIS, K.-C., 2010: Nitrogen cycling in the German Bight (SE North Sea)—Clues from modelling $\delta^{15}\text{N}$ nitrogen isotopes. *Continental Shelf Research*, **30**, 203–213.
- SCHMIDT, F., KOCH, B. P., GOLDHAMMER, T., ELVERT, M., WITT, M., LIN, Y.-S., WENDT, J., ZABEL, HINRICHS, K.-U., 2017: Unraveling signatures of biogeochemical processes and the depositional setting in the molecular composition of pore water DOM across different marine environments. *Geochimica et Cosmochimica Acta*, **207**, 57–80.
- SEITZINGER, S. P., SVEDIN, U., CRUMLEY, C. L., STEFFEN, W., ABDULLAH, S. A., ALFSEN, C., BROADGATE, W. J., BIERMANN, F., BONDRE, N. R., DEARING, J. A., DEUTSCH, L., DHAKAL, S., ELMQVIST, T., FARAHBAKSHAZAD, N., GAFFNEY, O., HABERL, H., LAVOREL, S., MBOW, C., MCMICHAEL, A. J., DEMORAIS, J. M., OLSSON, P., PINHO, P. F., SETO, K. C., SINCLAIR, P., STAFFORD SMITH, M., SUGAR, L., 2012: Planetary stewardship in an urbanizing world: beyond city limits. *Ambio*, **41**(8), 787–794.
- SHI, Z., LIU, K., ZHANG, S., XU, H., LIU, H., 2019: Spatial distributions of mesozooplankton biomass, community composition and grazing impact in association with hypoxia in the Pearl River Estuary, *Estuarine, Coastal and Shelf Science*, **225**, 106237.

- SIGMAN, D. M., GRANGER, J., DIFIORE, P. J., LEHMANN, M. M., HO, R., CANE, G., VAN GEEN, A., 2005: Coupled nitrogen and oxygen isotope measurements of nitrate along the eastern North Pacific margin. *Global Biogeochemical Cycles*, **19**, GB4022.
- SIMON-DELISO, N., AMARAL-ROGERS, V., BELZUNCES, L. P., BONMATIN, J. M., CHAGNON, M., DOWNS, C., FURLAN, L., GIBBONS, D.W., GIORIO, C., GIROLAMI, V., GOULSON, D., KREUTZWEISER, D. P., KRUPKE, C. H., LIESS, M., LONG, E., MCFIELD, M., MINEAU, P., MITCHELL, E. A. D., MORRISSEY, C. A., NOOME, D. A., PISA, L., SETTELE, J., STARK, J. D., TAPPARO, A., VAN DYCK, H., VAN PRAAGH, J., VAN DER SLUIJS, J. P., WHITEHORN, P. R., WIEMERS, M., 2015: Systemic insecticides (neonicotinoids and fipronil): Trends, uses, mode of action and metabolites. *Environmental Science and Pollution Research*, **22**(1), 5–34.
- SZAREK, R., KUHN, W., KAWAMURA, H., KITAZATO, H., 2006: Distribution of recent benthic foraminifera on the Sunda Shelf (South China Sea). *Marine Micropaleontology*, **61**(4), 171–195.
- SZAREK, R., KUHN, W., KAWAMURA, H., NISHI, H., 2009: Distribution of recent foraminifera along continental slope of the Sunda Shelf (South China Sea). *Marine Micropaleontology*, **71**(1–2), 41–59.
- TANG, C., ZHOU, D., ENDLER, R., LIN, J., HARFF, J., 2010: Sedimentary development of the Pearl River Estuary based on seismic stratigraphy. *Journal of Marine Systems*, **82**, suppl. 1, S3–S16.
- TANG, D., LIU, X., ZOU, X., 2018: An improved method for integrated ecosystem health assessments based on the structure and function of coastal ecosystems: A case study of the Jiangsu coastal area, China. *Ecological Indicators*, **84**, 82–95.
- TANG, D., LIU, X., HE, H., CUI, Z., GAN, H., XIA, Z., 2020: Distribution, sources and ecological risks of organochlorine compounds (DDTs, HCHs and PCBs) in surface sediments from the Pearl River Estuary, China. *Marine Pollution Bulletin*, **152**, 110942.
- TU, C., CHEN, T., ZHOU, Q., LIU, Y., WEI, J., WANIEK, J. J., LUO, Y., 2020: Biofilm formation and its influences on the properties of microplastics as affected by exposure time and depth in the seawater. *Science of The Total Environment*, **734**, 139237.
- UNESCO, 2016: Water Megacities and Global Change: Portraits of 15 Emblematic Cities of the World. UNESCO Reports.
- WAN, S., ZHIMIN, J., 2014: Deep water exchanges between the South China Sea and the Pacific since the last glacial period. *Paleoceanography and Paleoclimatology*, **29**(12), 1162–1178.
- WANG, N., HUANG, B.-Q., DONG, Y.-T., XIE, X., 2018: The evolution of deepwater dissolved oxygen in the northern South China Sea since 400 ka. *Palaeoworld*, **27**(2), 301–308.
- WEI, X., WU, C. Y., 2011: Holocene delta evolution and sequence stratigraphy of the Pearl River Delta in South China. *Science China Earth Sciences*, **54**, 1523.
- WEISHAAR, J. L., AIKEN, G. R., BERGAMASCHI, B. A., FRAM, M. S., FUJII, R., MOPPER, K., 2003: Evaluation of specific ultraviolet absorbance as an indicator of the chemical composition and

- reactivity of dissolved organic carbon. *Environmental Science and Technology*, **37**(20), 4702–4708.
- XU, Y., HE, H., SONG, J., HOU, Y., LI, F., 2017: Observations and modeling of typhoon waves in the South China Sea. *Journal of Physical Oceanography*, **47**(6), 1307–1324.
- YANG, J.-Y. T., KAO, S.-J., DAI, M., YAN, X., LIN, H.-L., 2017: Examining N cycling in the northern South China Sea from N isotopic signals in nitrate and particulate phases. *Journal of Geophysical Research: Biogeosciences*, **122**(8), 2118–2136.
- YE, F., NI, Z., XIE, L., WEI, G., JIA, G., 2015: Isotopic evidence for the turnover of biological reactive nitrogen in the Pearl River Estuary, south China. *Journal of Geophysical Research: Biogeosciences*, **120**(4), 662–672.
- YING, G.-G., KOOKANA, R. S., KUMAR, A., 2008: Fate of estrogens and xenoestrogens in four sewage treatment plants with different technologies. *Environmental Toxicology and Chemistry*, **27**(1), 87–94.
- YING, G.-G., KOOKANA, R. S., RU, Y.-J., 2002: Occurrence and fate of hormone steroids in the environment. *Environment International*, **28**(6), 545–551.
- YOUNG, I. R., 2006: Directional spectra of hurricane wind waves. *Journal of Geophysical Research*, **111**(C8), C08020.
- ZHANG, J., YU, Z., RAABE, T., LIU, S., STARKE, A., ZOU, L., GAO, H., BROCKMANN, U., 2004: Dynamics of inorganic nutrient species in the Bohai Sea waters. *Journal of marine systems*, **44**, 189–212.
- ZHANG, W., SUN, X., ZHENG, S., ZHU, M., LIANG, J., DU, J., YANG, C., 2019: Plankton abundance, biovolume, and normalized biovolume size spectra in the northern slope of the South China Sea in autumn 2014 and summer 2015. *Deep Sea Research Part II: Topical Studies in Oceanography*, **167**, 79–92.
- ZHANG, W., TANG, D., YANG, B., GAO, S., SUN, J., TAO, Z., SUN, S., NING, X., 2009: Onshore–offshore variations of copepod community in northern South China Sea. *Hydrobiologia*, **636**, 257–269.
- ZHAO, L., WEI, H., FENG, S., 2002: [Annual cycle and budgets of nutrients in the Bohai Sea]. *Huan Jing ke Xue= Huanjing Kexue*, **23**(1), 78–81.
- ZHAO, S., LIU, Z., COLIN, C., ZHAO, Y., WANG, X., JIAN, Z., 2018: Responses of the East Asian Summer Monsoon in the Low-Latitude South China Sea to High-Latitude Millennial-Scale Climatic Changes During the Last Glaciation: Evidence From a High-Resolution Clay Mineralogical Record. *Paleoceanography and Paleoclimatology*, **33**(7), 745–765.
- ZHEN, X., TANG, J., LIU, L., WANG, X., LI, Y., XIE, Z., 2018: From headwaters to estuary: Distribution and fate of halogenated flame retardants (HFRs) in a river basin near the largest HFR manufacturing base in China. *Science of The Total Environment*, **621**, 1370–1377.
- ZHOU, L. B., HUANG, L. M., TAN, Y. H., LIAN, X. P., LI, K. Z., 2015: Size-based analysis of a zooplankton community under the influence of the Pearl River plume and coastal upwelling in the northeastern South China Sea. *Marine Biology Research*, **11**, 168–179.

ZHOU, Q., TU, C., FU, C., LI, Y., ZHANG, H., XIONG, K., ZHAO, X., LI, L., WANIEK, J. J. LUO, Y., 2020: Characteristics and distribution of microplastics in the coastal mangrove sediments of China. *Science of the Total Environment*, **703**, 134807.

Waniek, J.J., Schulz-Bull, D.E., Gaye, B., Ebinghaus, R., Kunz, F., Pohlmann, T., Emeis, K.-C. (eds.): Megacity's fingerprint in Chinese marginal seas.

CONTENT

Kurzfassung

Summary

1 Preface

2 Physical forcing and the pattern of emerging pollutants in South China Sea

3 Investigations of pollutants dispersal in the Bohai and Yellow Sea

4 Comparison of the European and Asian marginal seas

5 Conclusions and outlook

Acknowledgements

References

